

# Shape coexistence and collective low-spin states in $^{112,114}\text{Sn}$ (Lifetime measurements with SONIC@HORUS)

M. Spieker *et al.*, PRC **97**, 054319 (2018)

Mark Spieker<sup>1,2</sup>, P. Petkov<sup>2,3</sup>, S. G. Pickstone<sup>2</sup>, S. Prill<sup>2</sup>, P. Scholz<sup>2</sup>, and A. Zilges<sup>2</sup>

<sup>1</sup> NSCL, Michigan State University, East Lansing, MI 48824, USA

<sup>2</sup> Institute for Nuclear Physics, University of Cologne, Germany

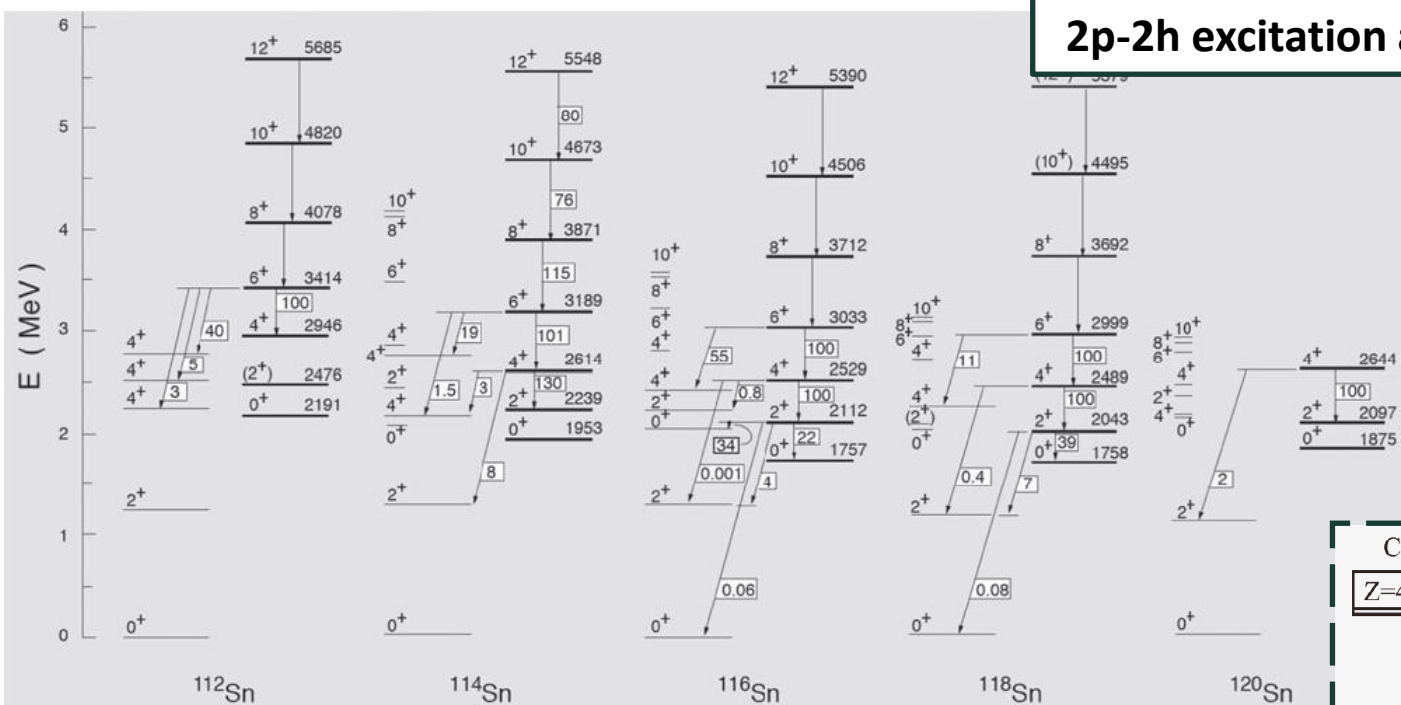
<sup>3</sup>IFIN-HH, Bucharest, Romania



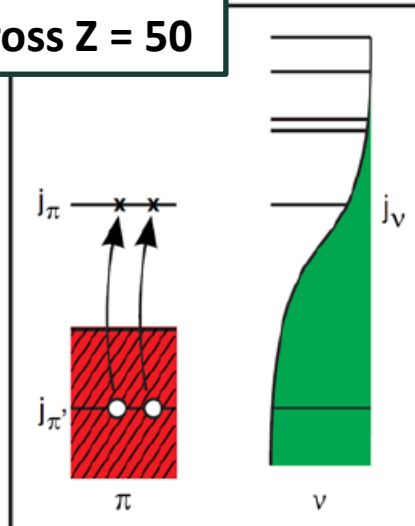
supported by



# Shape coexistence in Z = 50 region



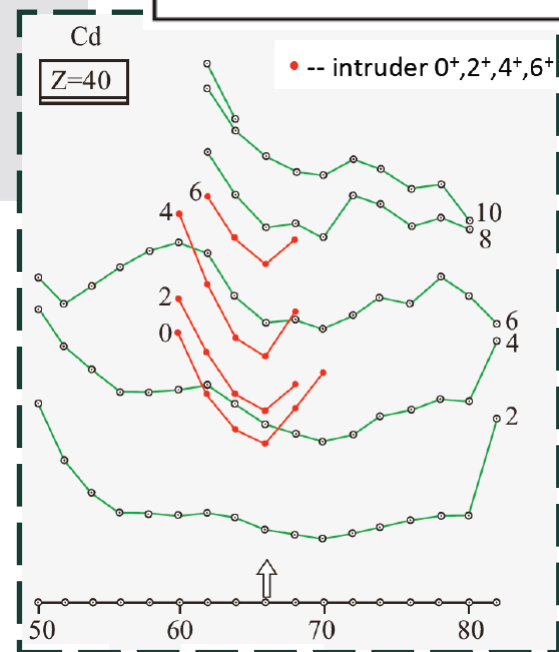
## 2p-2h excitation across Z = 50



## “additional” states observed

→ attributed to 2p-2h excitations across the Z = 50 shell closure, i.e. Pd isotopes as “inert core”

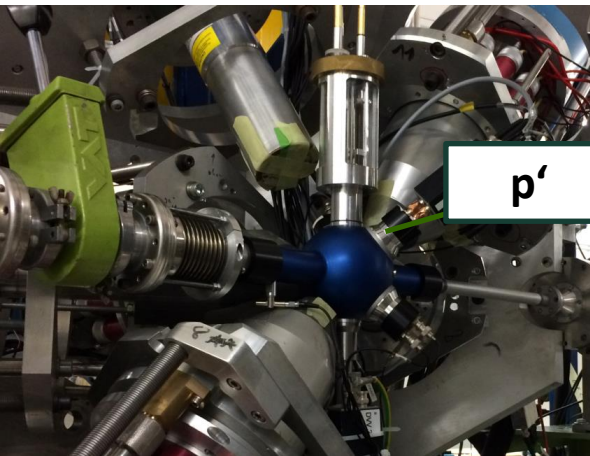
**Figures:**  
 P.E. Garrett, SSNET17  
 D. Rowe and J.L. Wood, *Models of Nuclear Structure: Foundational Models* (World Scientific, Singapore, 2010)



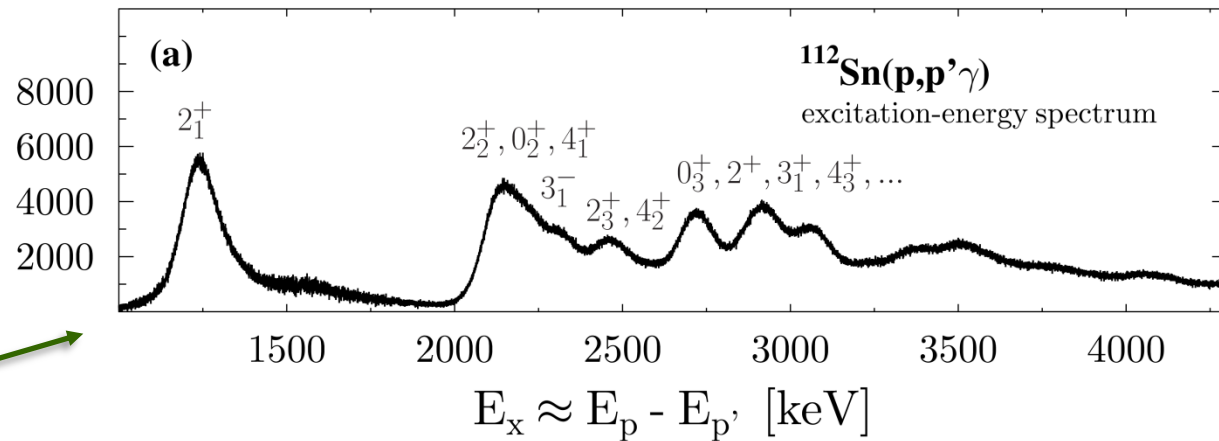


# (p,p'γ) DSA coincidence technique

SONIC@HORUS



counts / 0.25 keV

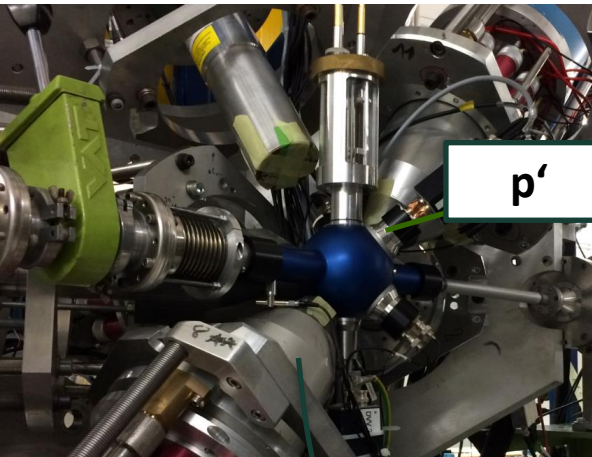


(p,p'γ) DSA coincidence technique: A. Hennig *et al.*, NIM **794**, 171 (2015)

SONIC@HORUS (UoC, Germany): S.G. Pickstone *et al.*, NIM **875**, 104 (2017)

# (p,p'γ) DSA coincidence technique

SONIC@HORUS

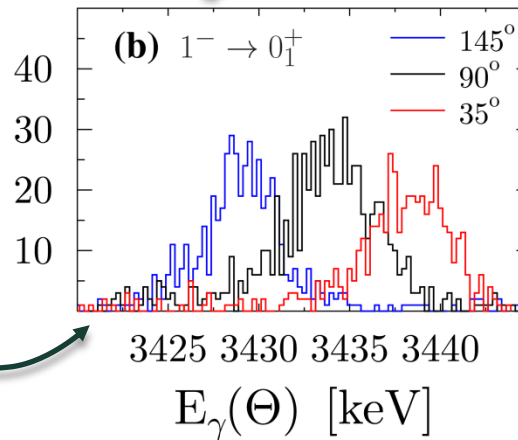
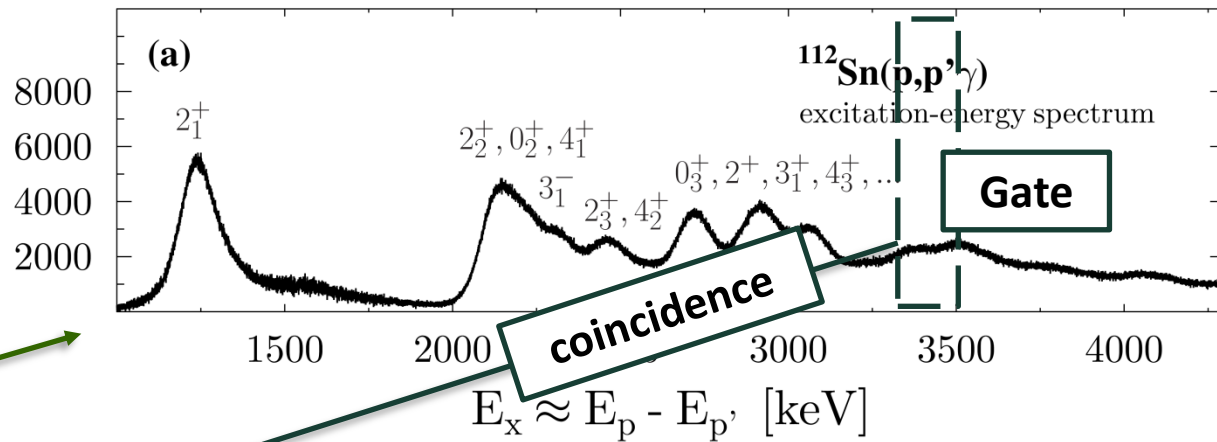


p'

γ

counts / 0.25 keV

counts / 0.25 keV

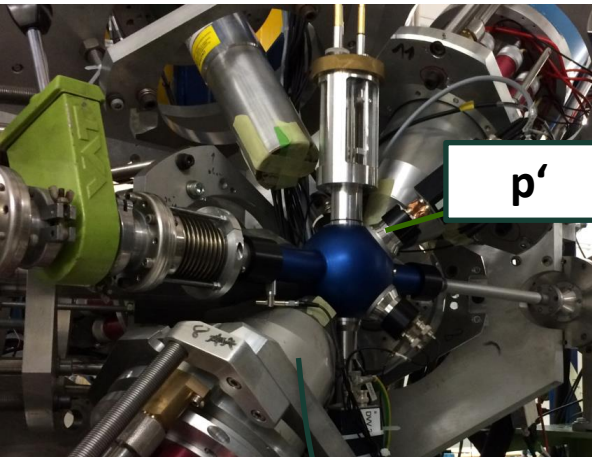


(p,p'γ) DSA coincidence technique: A. Hennig *et al.*, NIM **794**, 171 (2015)

SONIC@HORUS (UoC, Germany): S.G. Pickstone *et al.*, NIM **875**, 104 (2017)

# (p,p'γ) DSA coincidence technique

SONIC@HORUS

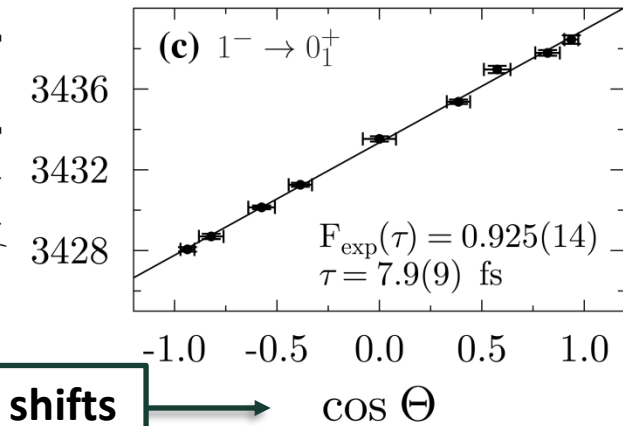
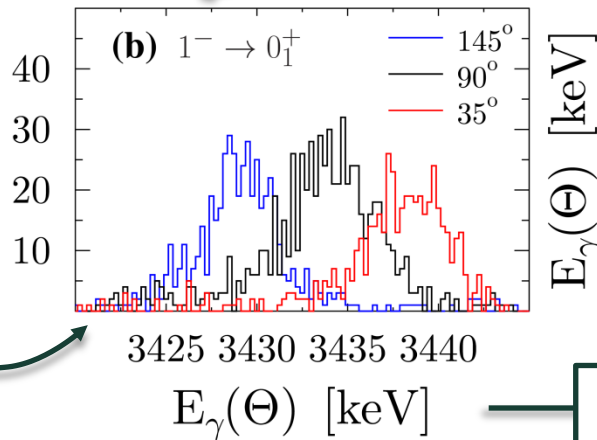
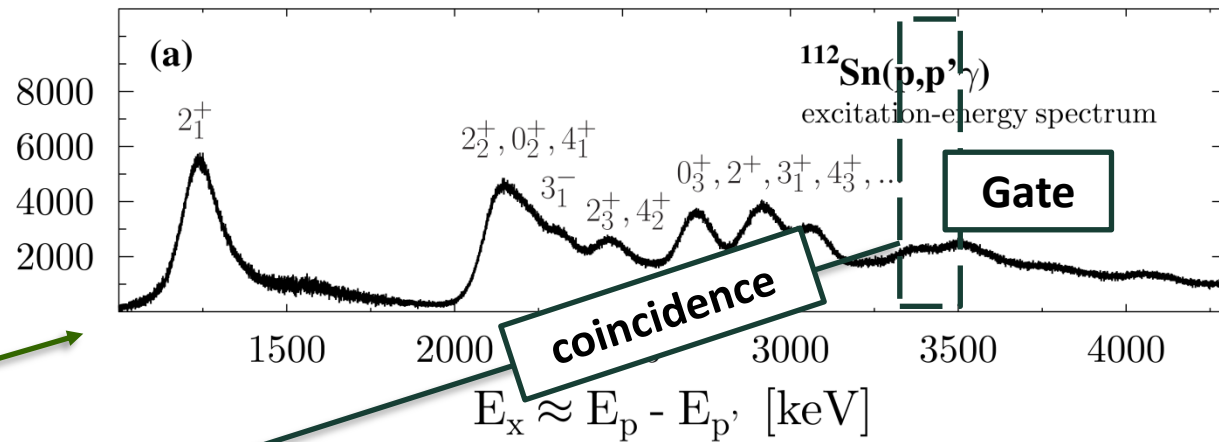


p'

γ

counts / 0.25 keV

counts / 0.25 keV

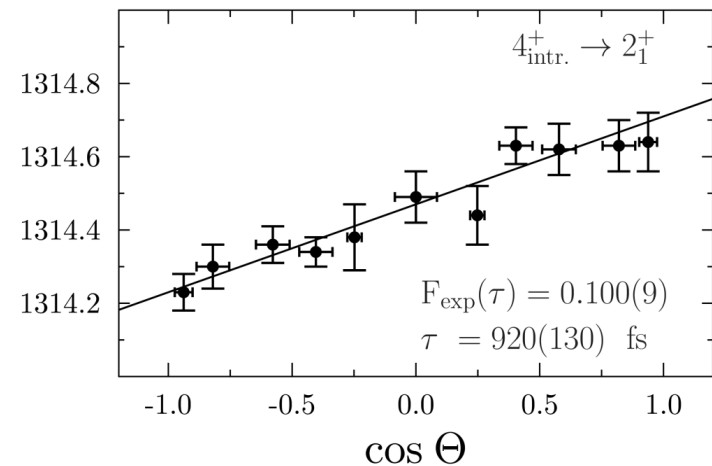
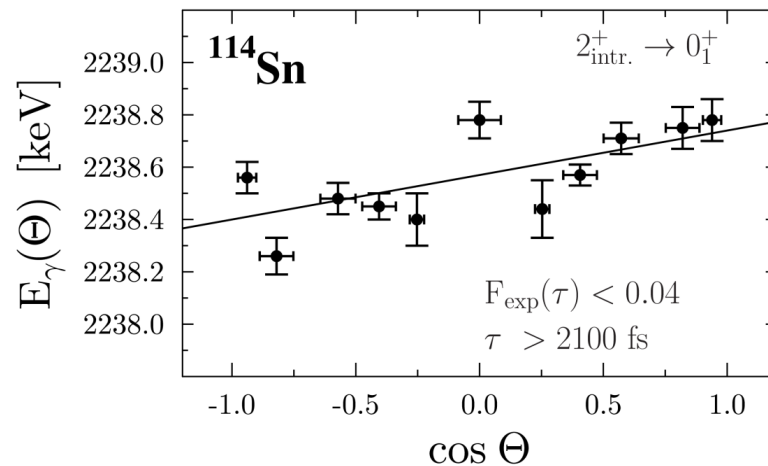
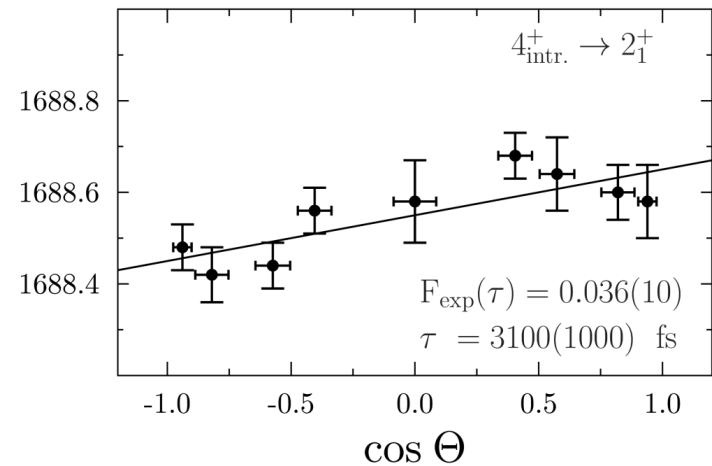
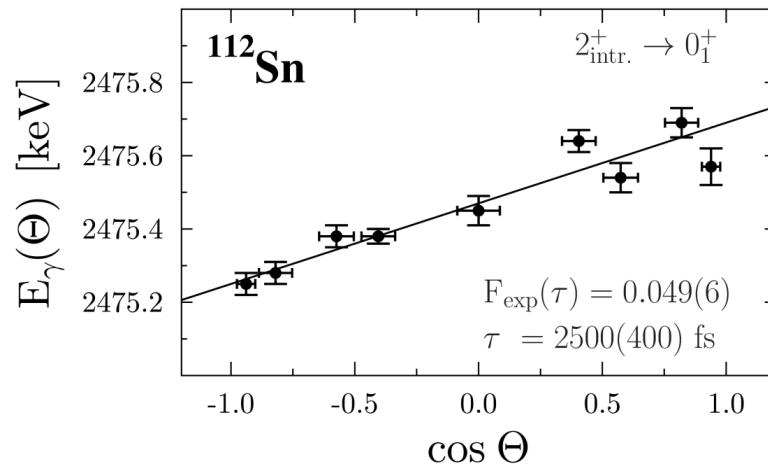


(p,p'γ) DSA coincidence technique: A. Hennig *et al.*, NIM **794**, 171 (2015)

SONIC@HORUS (UoC, Germany): S.G. Pickstone *et al.*, NIM **875**, 104 (2017)



# Lifetimes of intruder states in $^{112,114}\text{Sn}$



# $\gamma$ -decay behavior of the states of interest

## $^{112}\text{Sn}$

$E_x$ [keV]	$J_i^\pi$	$J_f^\pi$	$E_\gamma$ [keV]	$I_\gamma$ [%]
1256.5(2)	$2_1^+$	$0_1^+$	1256.5(2)	100
2150.5(3)	$2_2^+$	$0_1^+$	2150.5(2)	20(3)
	$2_2^+$	$2_1^+$	893.9(2)	100
2190.5(2)	$0_2^+$	$2_1^+$	934.0(2)	100
2247.0(3)	$4_1^+$	$2_1^+$	990.47(10)	100
2353.7(2)	$3_1^-$	$2_1^+$	1097.2(2)	100
2475.5(2)	$2_3^+$	$0_1^+$	2475.5(2)	100
	$2_3^+$	$2_1^+$	1218.9(2)	36(5)
	$2_3^+$	$0_2^+$	284.9(2)	0.70(10)
2520.5(2)	$4_2^+$	$2_1^+$	1264.0(2)	100
⋮				
2945.0(7)	$4^+$	$2_1^+$	1688.5(2)	100
	$4^+$	$2_2^+$	794.2(2)	5.4(10)
	$4^+$	$4_1^+$	697.9(2)*	<1.5
	$4^+$	$2_3^+$	469.5(2)	18(3)
	$4^+$	$4_2^+$	424.6(3)*	4.9(9)
	$4^+$	$6_1^+$	396.4(4)*	2.3(5)
	$4^+$	$4^+$	161.4(2)*	9(2)

## $^{114}\text{Sn}$

$E_x$ [keV]	$J_i^\pi$	$J_f^\pi$	$E_\gamma$ [keV]	$I_\gamma$ [%]
1299.7(2)	$2_1^+$	$0_1^+$	1299.7(2)	100
1952.9(2)	$0_2^+$	$2_1^+$	653.2(2)	100
2155.9(2)	$0_3^+$	$2_1^+$	856.2(2)	100
2187.3(3)	$4_1^+$	$2_1^+$	887.6(2)	100
2238.6(2)	$2_2^+$	$0_1^+$	2238.5(2)	100
	$2_2^+$	$2_1^+$	938.9(2)	81(12)
	$2_2^+$	$0_2^+$	286.5(10)	0.9(3)
2274.5(2)	$3_1^-$	$2_1^+$	974.8(2)	100
2420.5(2)	$0_4^+$	$2_1^+$	1120.8(2)	100
2453.8(2)	$2_3^+$	$0_1^+$	2453.7(2)	28(4)
	$2_3^+$	$2_1^+$	1154.0(2)	100
	$2_3^+$	$2_2^+$	215.4(4)	1.3(3)
2514.4(2)	$3_1^+$	$4_1^+$	327.1(2)	100
2613.7(4)	$4_2^+$	$2_1^+$	1314.5(2)	100
	$4_2^+$	$4_1^+$	426.0(4)	1.6(6)
	$4_2^+$	$2_2^+$	375.2(3)	1.8(6)



# $\gamma$ -decay behavior of the states of interest

## $^{112}\text{Sn}$

$E_x$ [keV]	$J_i^\pi$	$J_f^\pi$	$E_\gamma$ [keV]	$I_\gamma$ [%]
1256.5(2)	$2_1^+$	$0_1^+$	1256.5(2)	100
2150.5(3)	$2_2^+$	$0_1^+$	2150.5(2)	20(3)
	$2_2^+$	$2_1^+$	893.9(2)	100
2190.5(2)	$0_2^+$	$2_1^+$	934.0(2)	100
2247.0(3)	$4_1^+$	$2_1^+$	990.47(10)	100
2353.7(2)	$3_1^-$	$2_1^+$	1097.2(2)	100
2475.5(2)	$2_3^+$	$0_1^+$	2475.5(2)	100
	$2_3^+$	$2_1^+$	1218.9(2)	36(5)
	$2_3^+$	$0_2^+$	284.9(2)	0.70(10)
2520.5(2)	$4_2^+$	$2_1^+$	1264.0(2)	100
⋮				
2945.0(7)	$4^+$	$2_1^+$	1688.5(2)	100
	$4^+$	$2_2^+$	794.2(2)	5.4(10)
	$4^+$	$4_1^+$	697.9(2)*	<1.5
	$4^+$	$2_3^+$	469.5(2)	18(3)
	$4^+$	$4_2^+$	424.6(3)*	4.9(9)
	$4^+$	$6_1^+$	396.4(4)*	2.3(5)
	$4^+$	$4^+$	161.4(2)*	9(2)

\* New  $\gamma$ -decay branching

## $^{114}\text{Sn}$

$E_x$ [keV]	$J_i^\pi$	$J_f^\pi$	$E_\gamma$ [keV]	$I_\gamma$ [%]
1299.7(2)	$2_1^+$	$0_1^+$	1299.7(2)	100
1952.9(2)	$0_2^+$	$2_1^+$	653.2(2)	100
2155.9(2)	$0_3^+$	$2_1^+$	856.2(2)	100
2187.3(3)	$4_1^+$	$2_1^+$	887.6(2)	100
2238.6(2)	$2_2^+$	$0_1^+$	2238.5(2)	100
	$2_2^+$	$2_1^+$	938.9(2)	81(12)
	$2_2^+$	$0_2^+$	286.5(10)	0.9(3)
2274.5(2)	$3_1^-$	$2_1^+$	974.8(2)	100
2420.5(2)	$0_4^+$	$2_1^+$	1120.8(2)	100
2453.8(2)	$2_3^+$	$0_1^+$	2453.7(2)	28(4)
	$2_3^+$	$2_1^+$	1154.0(2)	100
	$2_3^+$	$2_2^+$	215.4(4)	1.3(3)
2514.4(2)	$3_1^+$	$4_1^+$	327.1(2)	100
2613.7(4)	$4_2^+$	$2_1^+$	1314.5(2)	100
	$4_2^+$	$4_1^+$	426.0(4)	1.6(6)
	$4_2^+$	$2_2^+$	375.2(3)	1.8(6)

“intruder” states

# $\gamma$ -decay behavior of the states of interest

## $^{112}\text{Sn}$

$E_x$ [keV]	$J_i^\pi$	$J_f^\pi$	$E_\gamma$ [keV]	$I_\gamma$ [%]
1256.5(2)	$2_1^+$	$0_1^+$	1256.5(2)	100
2150.5(3)	$2_2^+$	$0_1^+$	2150.5(2)	20(3)
	$2_2^+$	$2_1^+$	893.9(2)	100
2190.5(2)	$0_2^+$	$2_1^+$	934.0(2)	100
2247.0(3)	$4_1^+$	$2_1^+$	990.47(10)	100
2353.7(2)	$3_1^-$	$2_1^+$	1097.2(2)	100
2475.5(2)	$2_3^+$	$0_1^+$	2475.5(2)	100
	$2_3^+$	$2_1^+$	1218.9(2)	36(5)
	$2_3^+$	$0_2^+$	284.9(2)	0.70(10)
2520.5(2)	$4_2^+$	$2_1^+$	1264.0(2)	100

### $0^+ @ 2617 \text{ keV}$

2945.0(7)	$4^+$	$2_1^+$	1688.5(2)	100
	$4^+$	$2_2^+$	794.2(2)	5.4(10)
	$4^+$	$4_1^+$	697.9(2)*	<1.5
	$4^+$	$2_3^+$	469.5(2)	18(3)
	$4^+$	$4_2^+$	424.6(3)*	4.9(9)
	$4^+$	$6_1^+$	396.4(4)*	2.3(5)
	$4^+$	$4^+$	161.4(2)*	9(2)

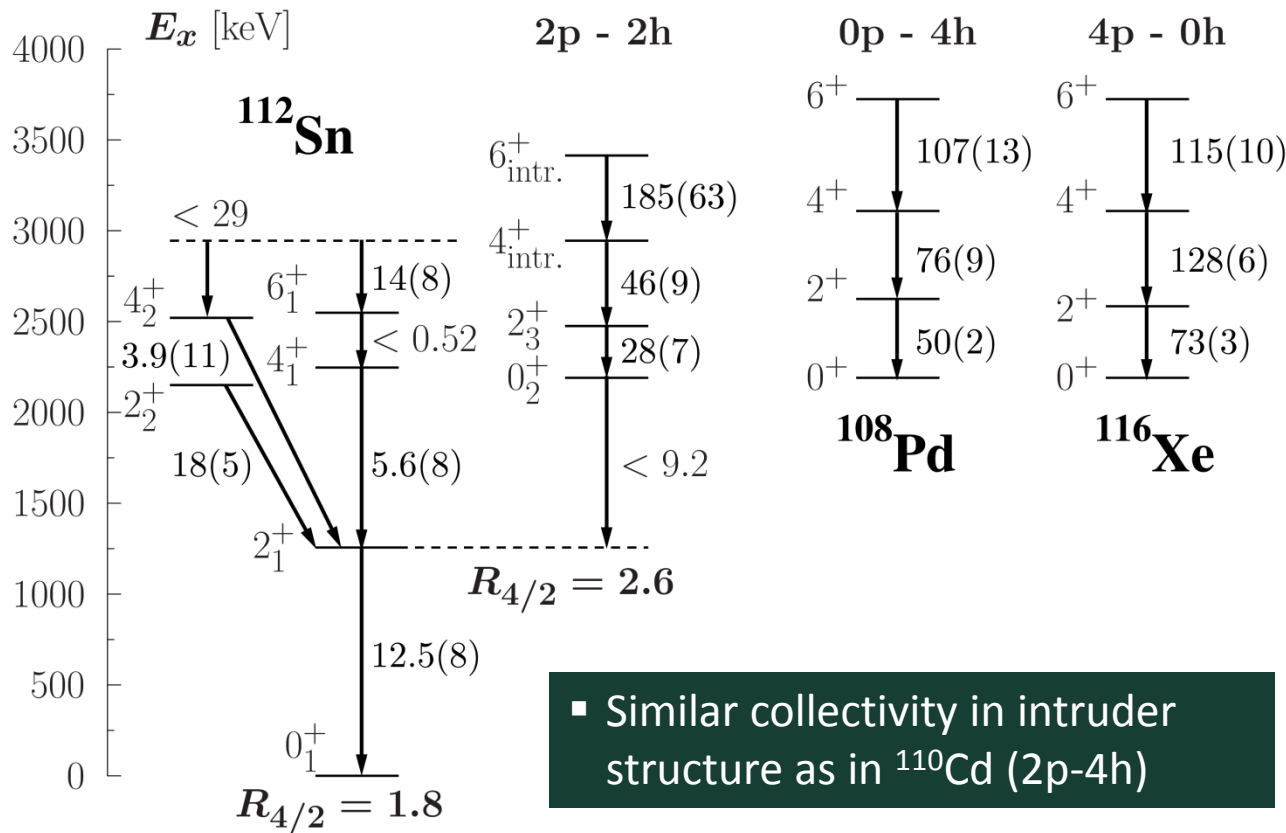
\* New  $\gamma$ -decay branching

## $^{114}\text{Sn}$

$E_x$ [keV]	$J_i^\pi$	$J_f^\pi$	$E_\gamma$ [keV]	$I_\gamma$ [%]
1299.7(2)	$2_1^+$	$0_1^+$	1299.7(2)	100
1952.9(2)	$0_2^+$	$2_1^+$	653.2(2)	100
2155.9(2)	$0_3^+$	$2_1^+$	856.2(2)	100
2187.3(3)	$4_1^+$	$2_1^+$	887.6(2)	100
2238.6(2)	$2_2^+$	$0_1^+$	2238.5(2)	100
	$2_2^+$	$2_1^+$	938.9(2)	81(12)
	$2_2^+$	$0_2^+$	286.5(10)	0.9(3)
2274.5(2)	$3_1^-$	$2_1^+$	974.8(2)	100
2420.5(2)	$0_4^+$	$2_1^+$	1120.8(2)	100
2453.8(2)	$2_3^+$	$0_1^+$	2453.7(2)	28(4)
	$2_3^+$	$2_1^+$	1154.0(2)	100
	$2_3^+$	$2_2^+$	215.4(4)	1.3(3)
2514.4(2)	$3_1^+$	$4_1^+$	327.1(2)	100
2613.7(4)	$4_2^+$	$2_1^+$	1314.5(2)	100
	$4_2^+$	$4_1^+$	426.0(4)	1.6(6)
	$4_2^+$	$2_2^+$	375.2(3)	1.8(6)

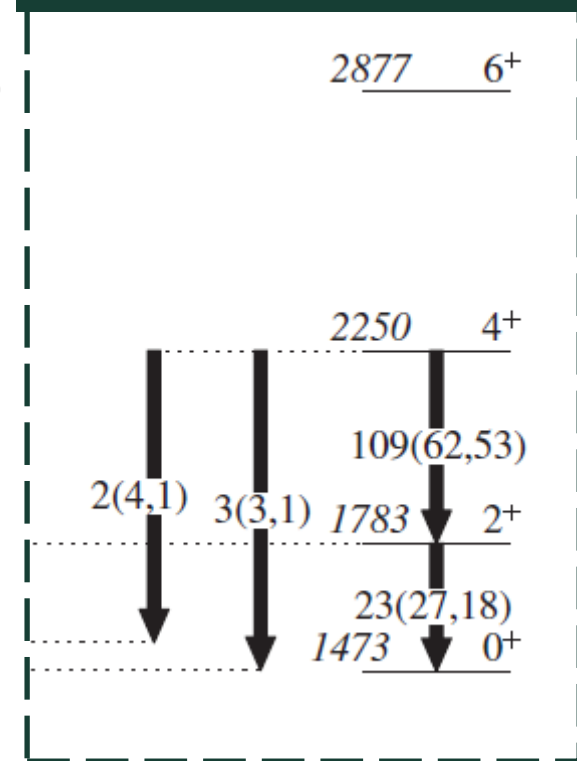
“intruder” states

# Shape coexistence in $^{112}\text{Sn}$

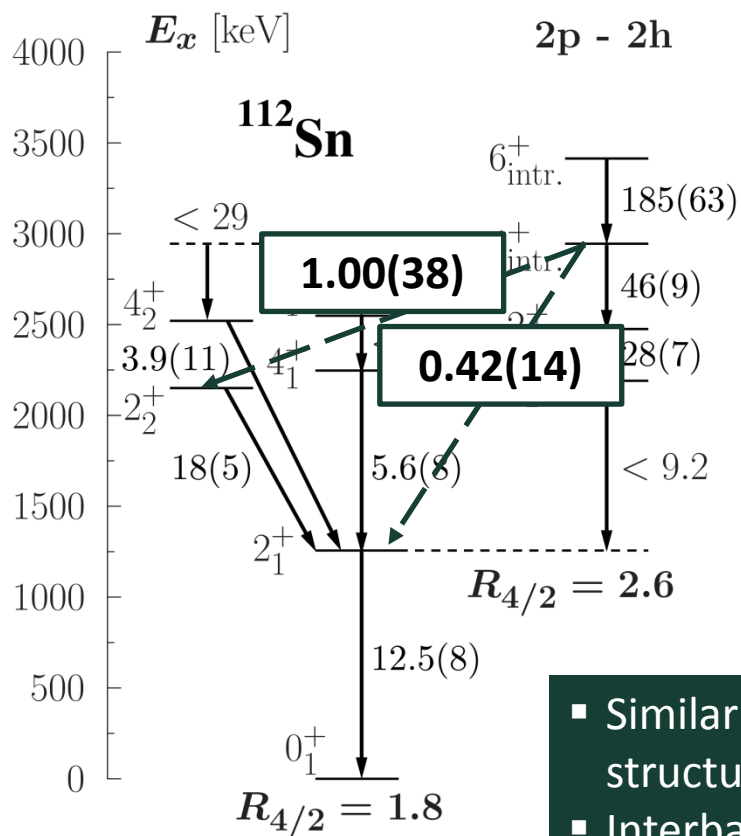


**$^{110}\text{Cd}$**

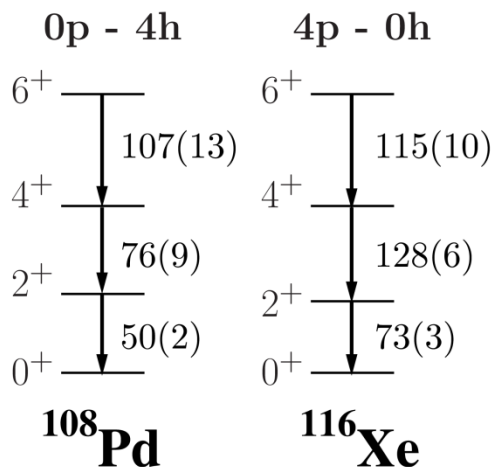
P.E. Garrett and J.L. Wood,  
J. Phys. G 37, 064028 (2010)



# Shape coexistence in $^{112}\text{Sn}$

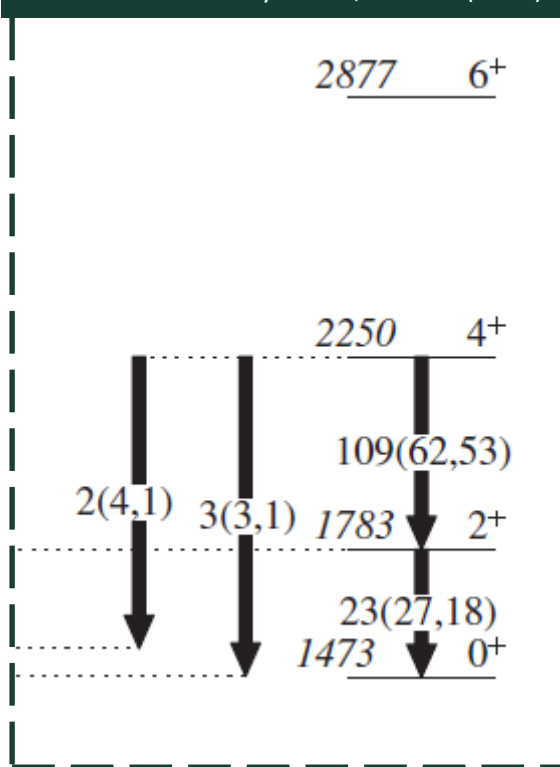


- Similar collectivity in intruder structure as in  $^{110}\text{Cd}$  (2p-4h)
- Interband transitions also weak

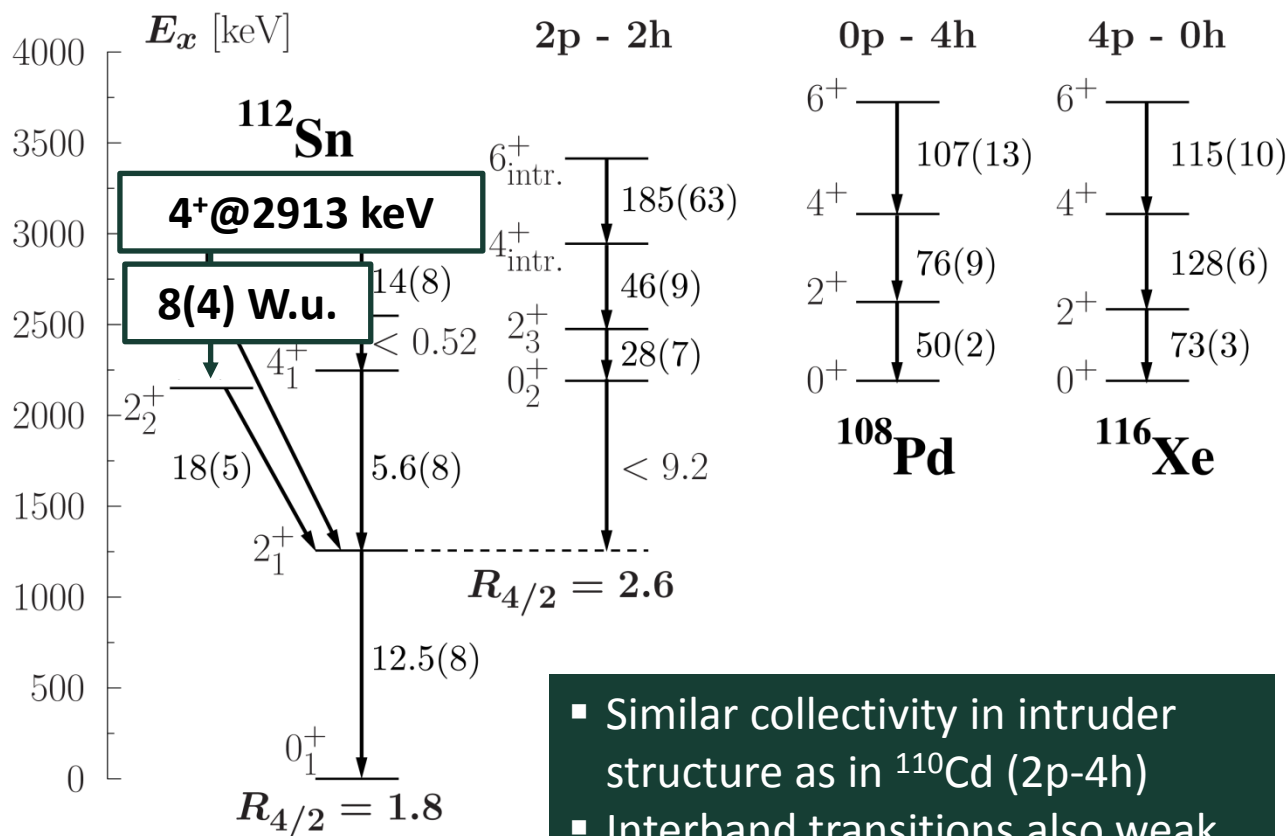


$^{110}\text{Cd}$

P.E. Garrett and J.L. Wood, J. Phys. G 37, 064028 (2010)



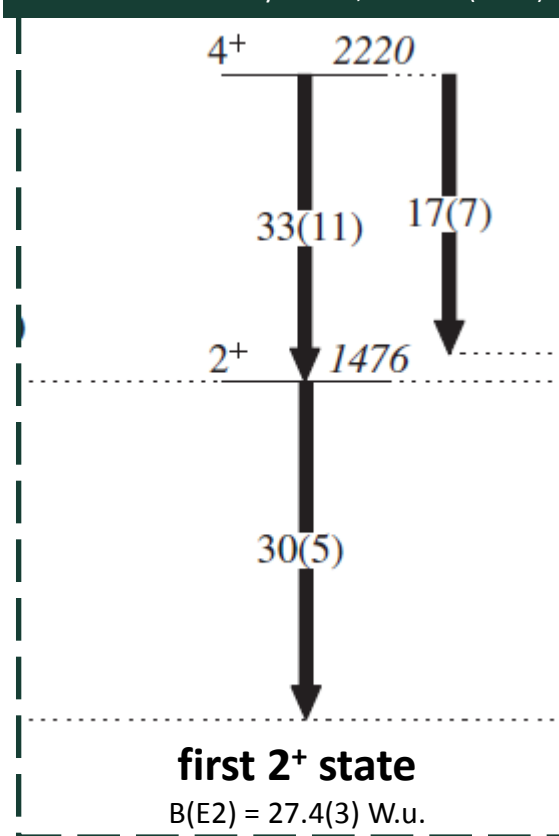
# Shape coexistence in $^{112}\text{Sn}$



- Similar collectivity in intruder structure as in  $^{110}\text{Cd}$  (2p-4h)
- Interband transitions also weak
- Quasi-rotational structure of Cd isotopes was proposed

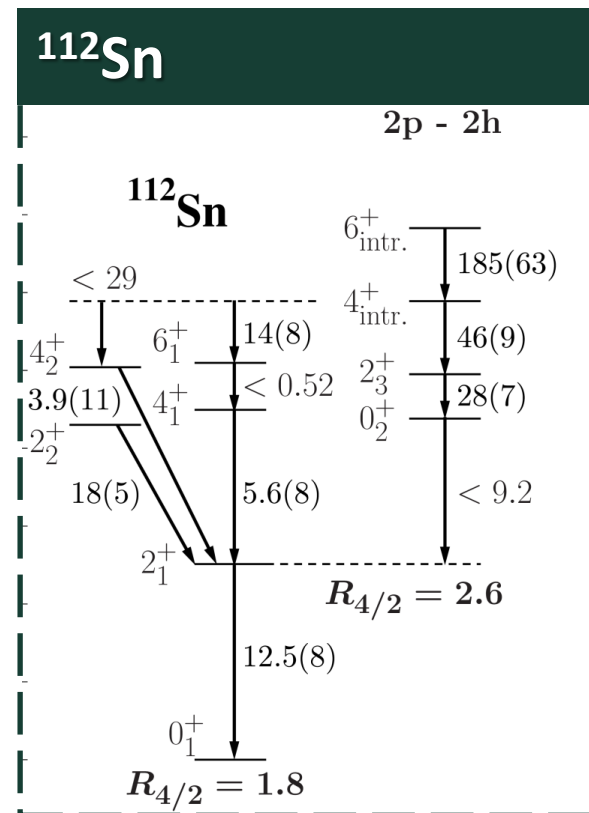
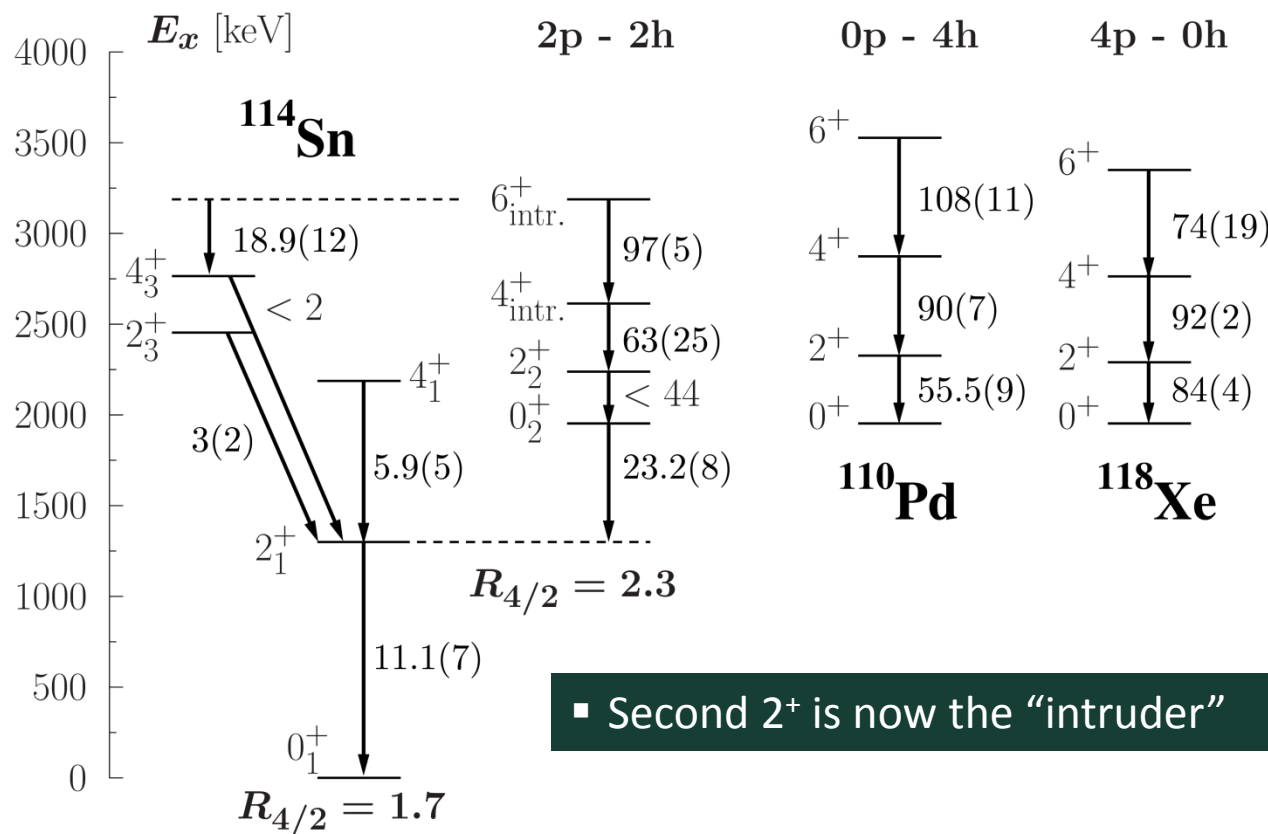
**$^{110}\text{Cd}$**

P.E. Garrett and J.L. Wood, J. Phys. G 37, 064028 (2010)



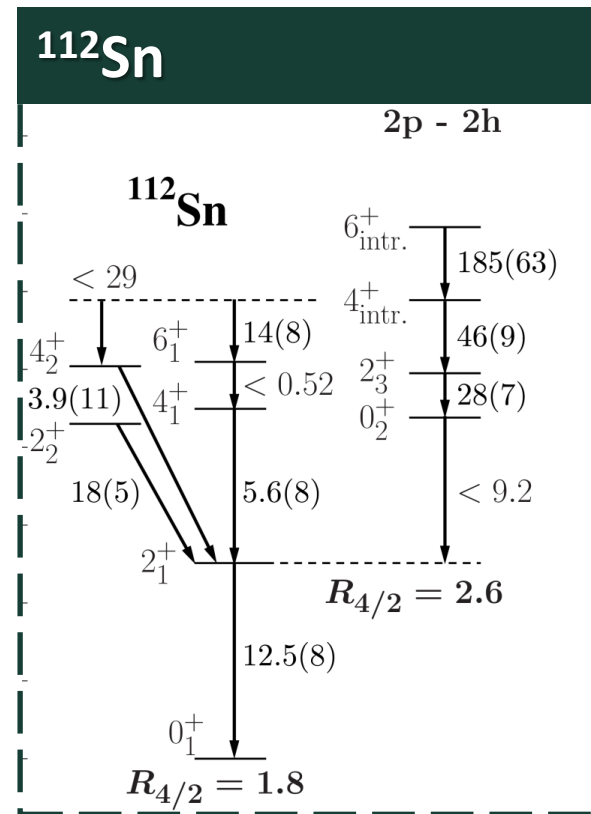
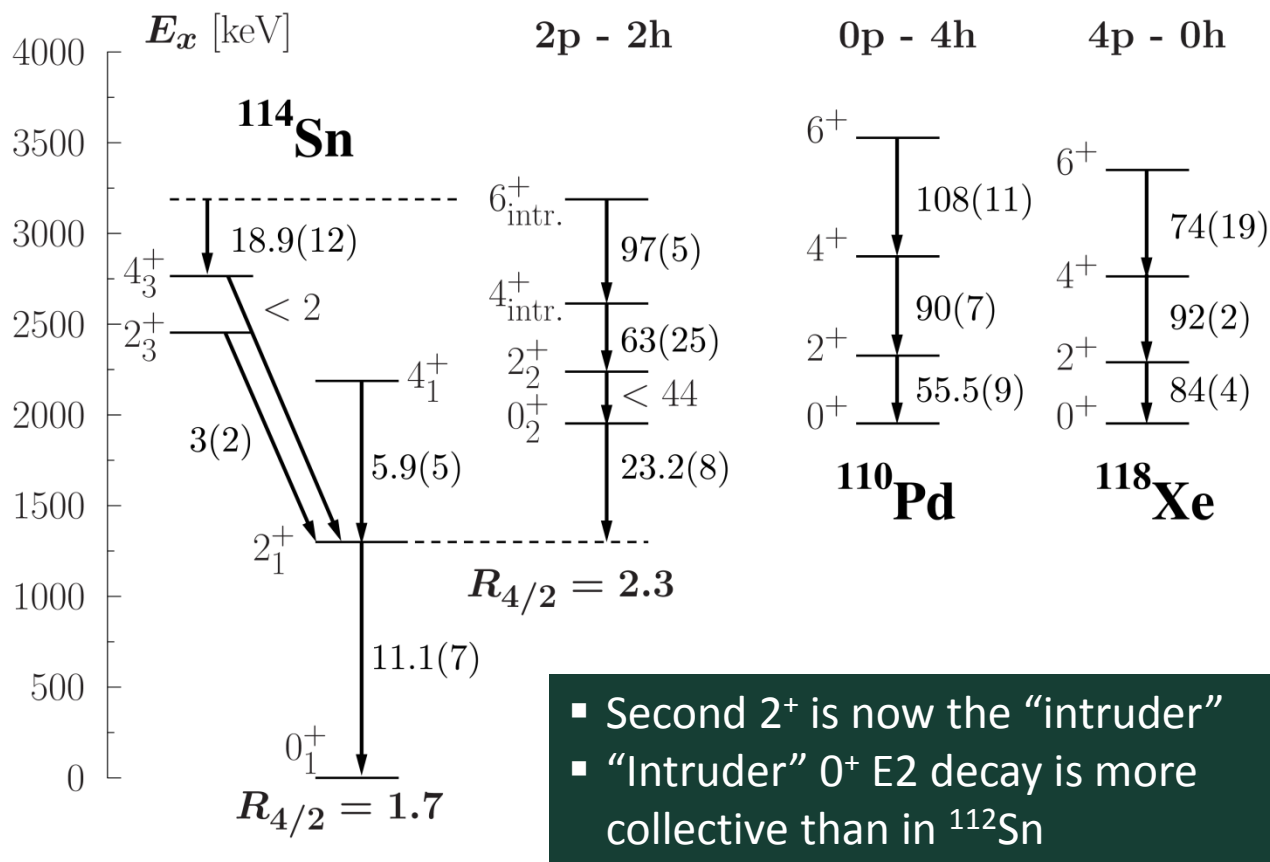
**“Quasi-rotational structure” already existent at higher energies in Sn isotopes?**

# Shape coexistence in $^{114}\text{Sn}$

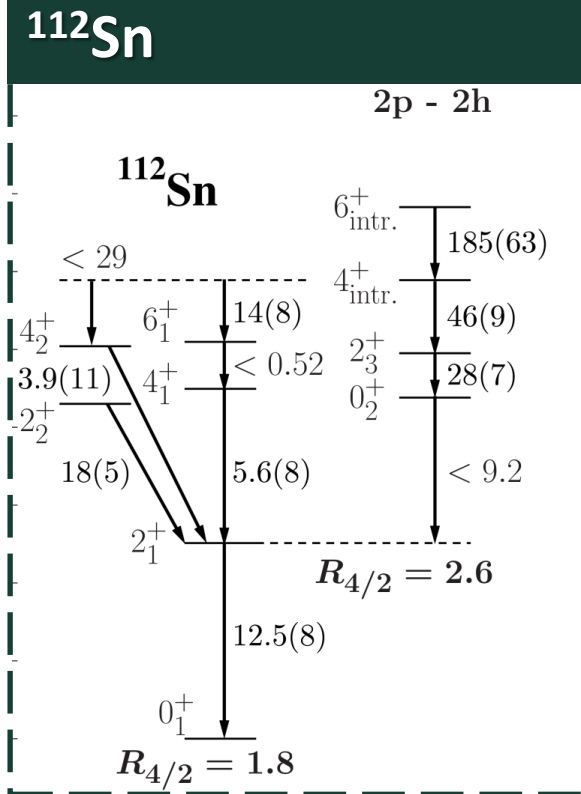
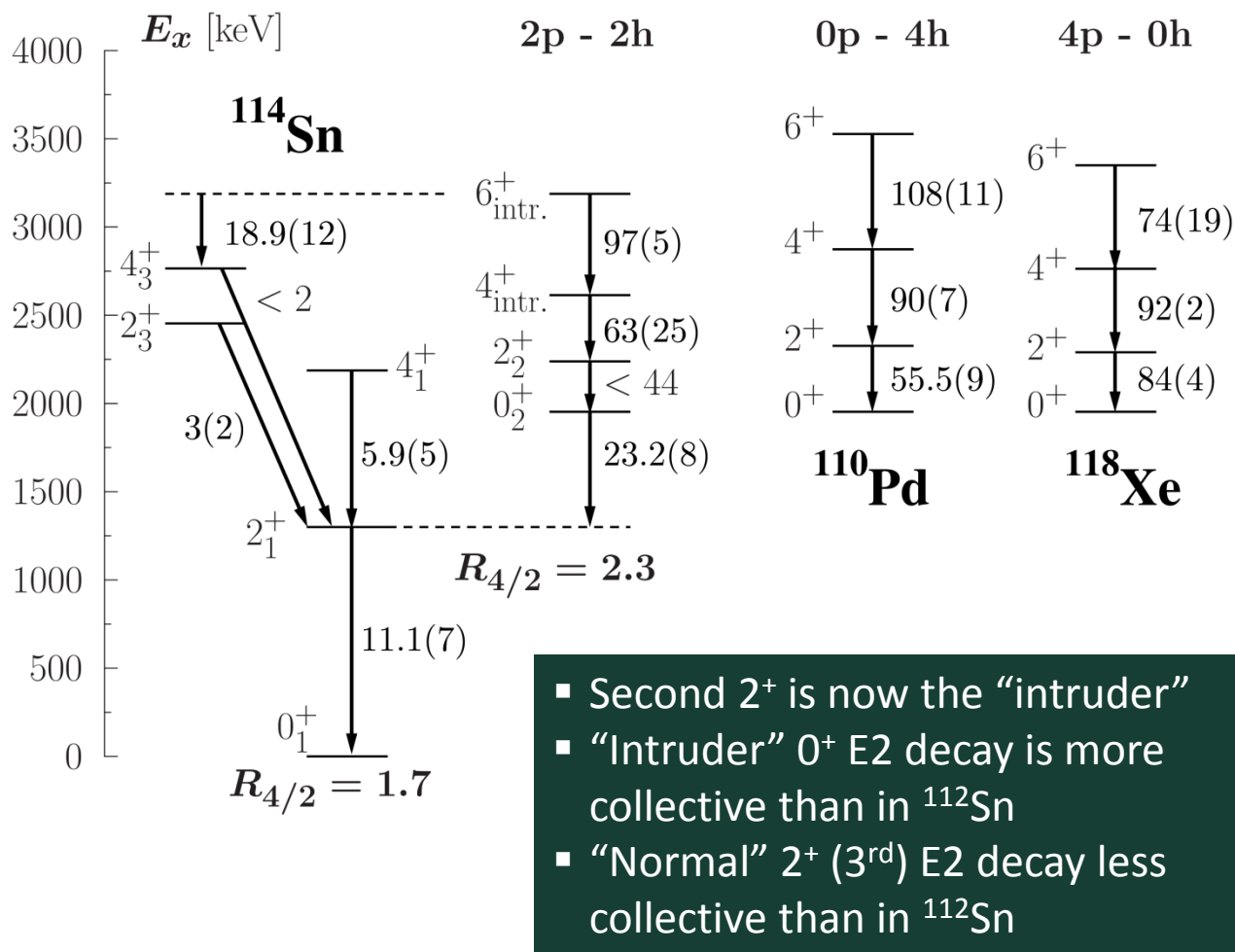




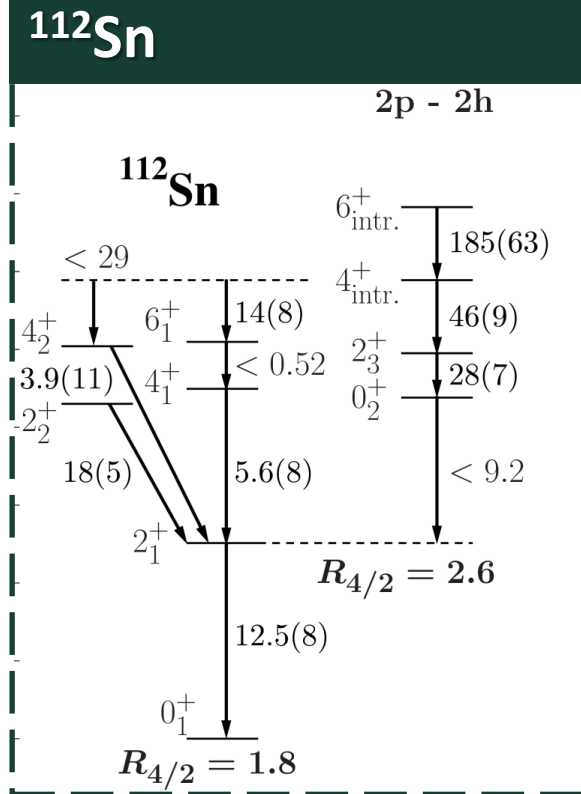
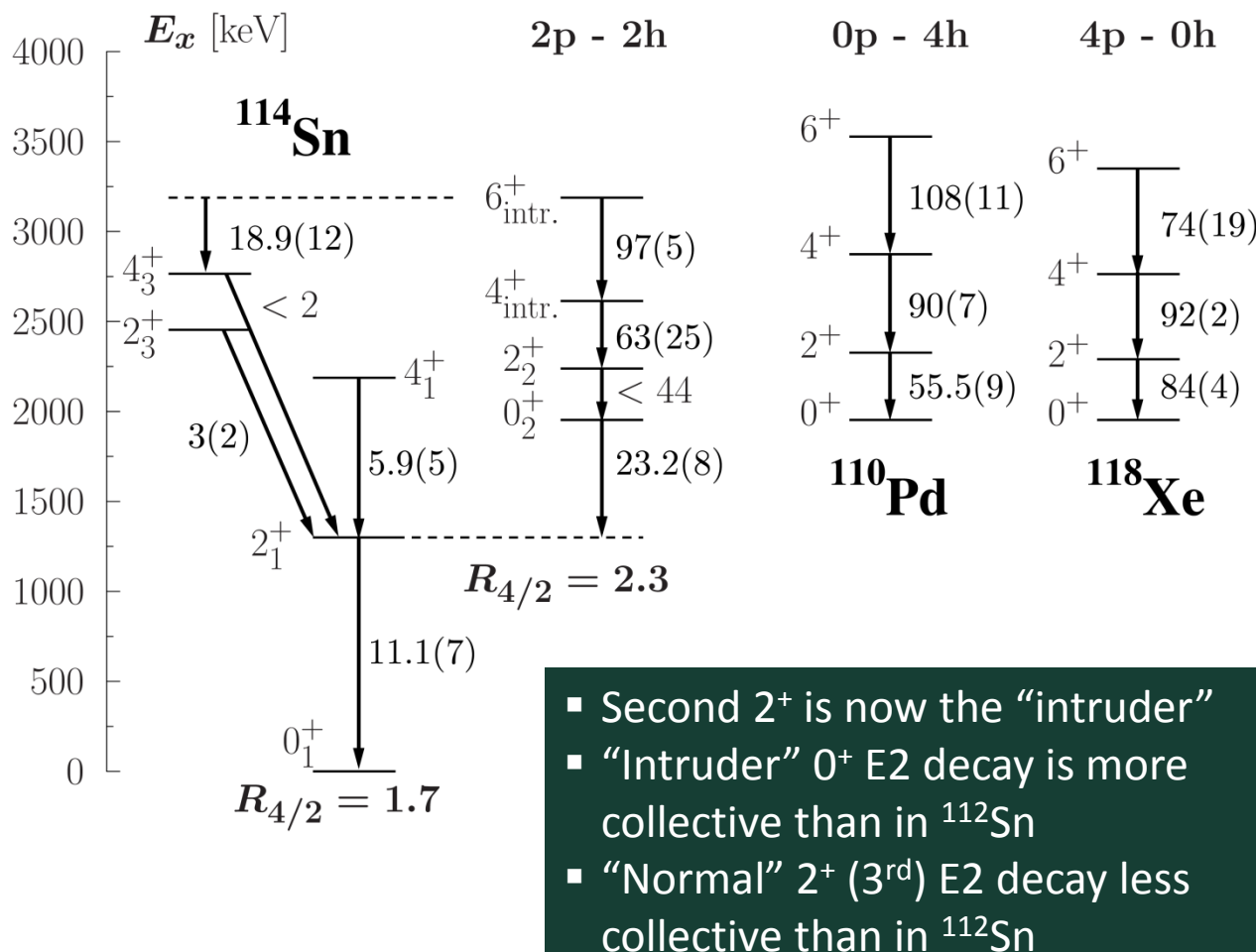
# Shape coexistence in $^{114}\text{Sn}$



# Shape coexistence in $^{114}\text{Sn}$



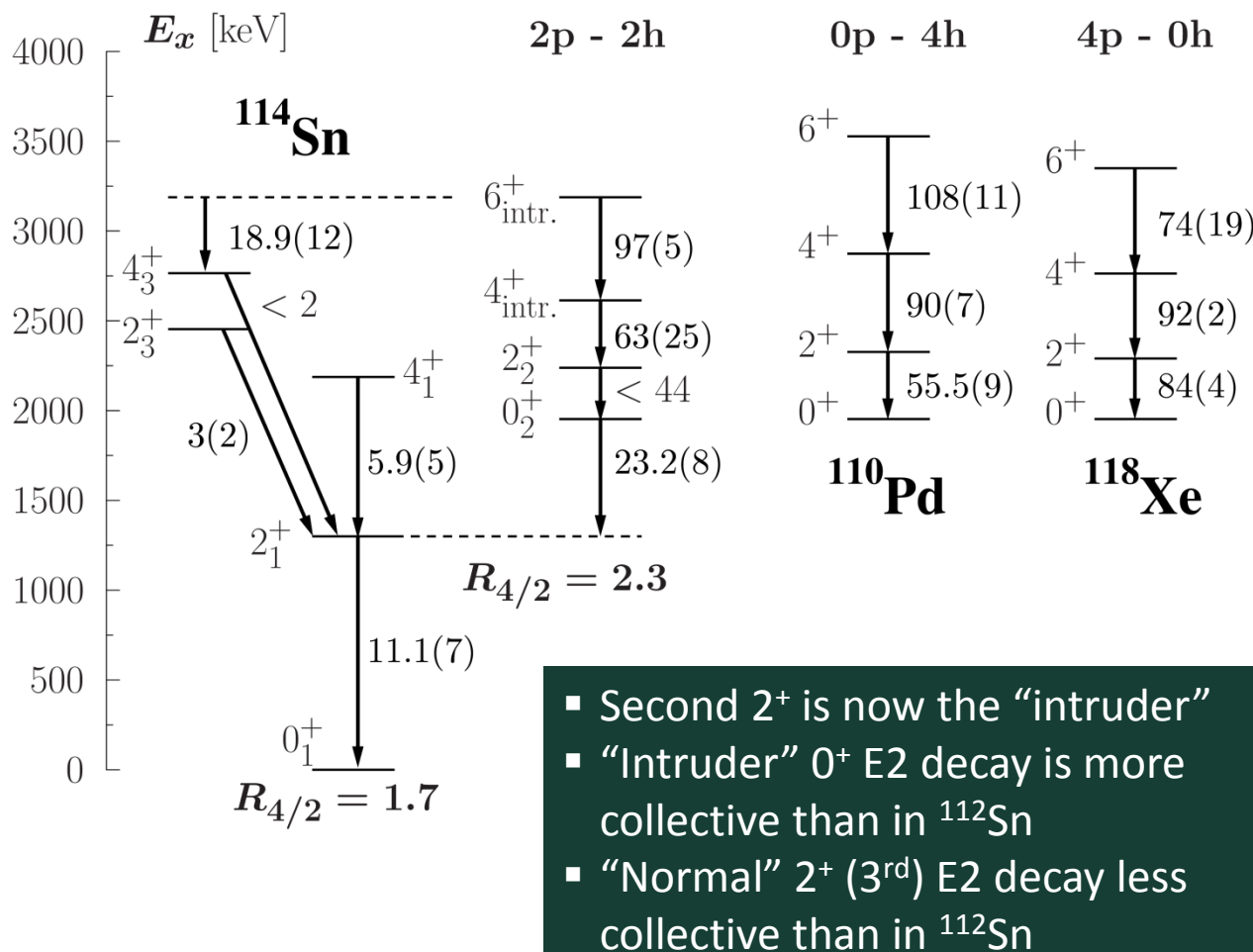
# Shape coexistence in $^{114}\text{Sn}$



**Influence of underlying single-particle structure or overall structure change?**

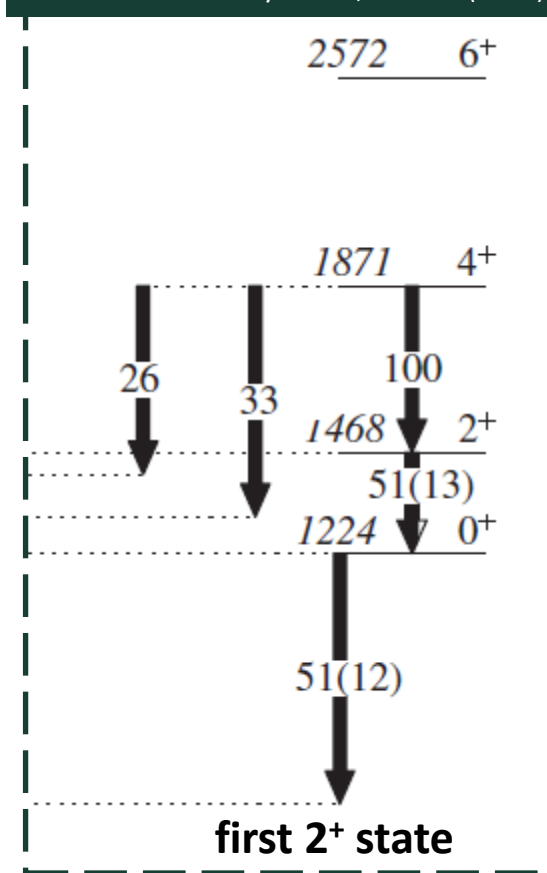
**Different influence of neutron single-particle states?**

# Shape coexistence in $^{114}\text{Sn}$



**$^{112}\text{Cd}$**

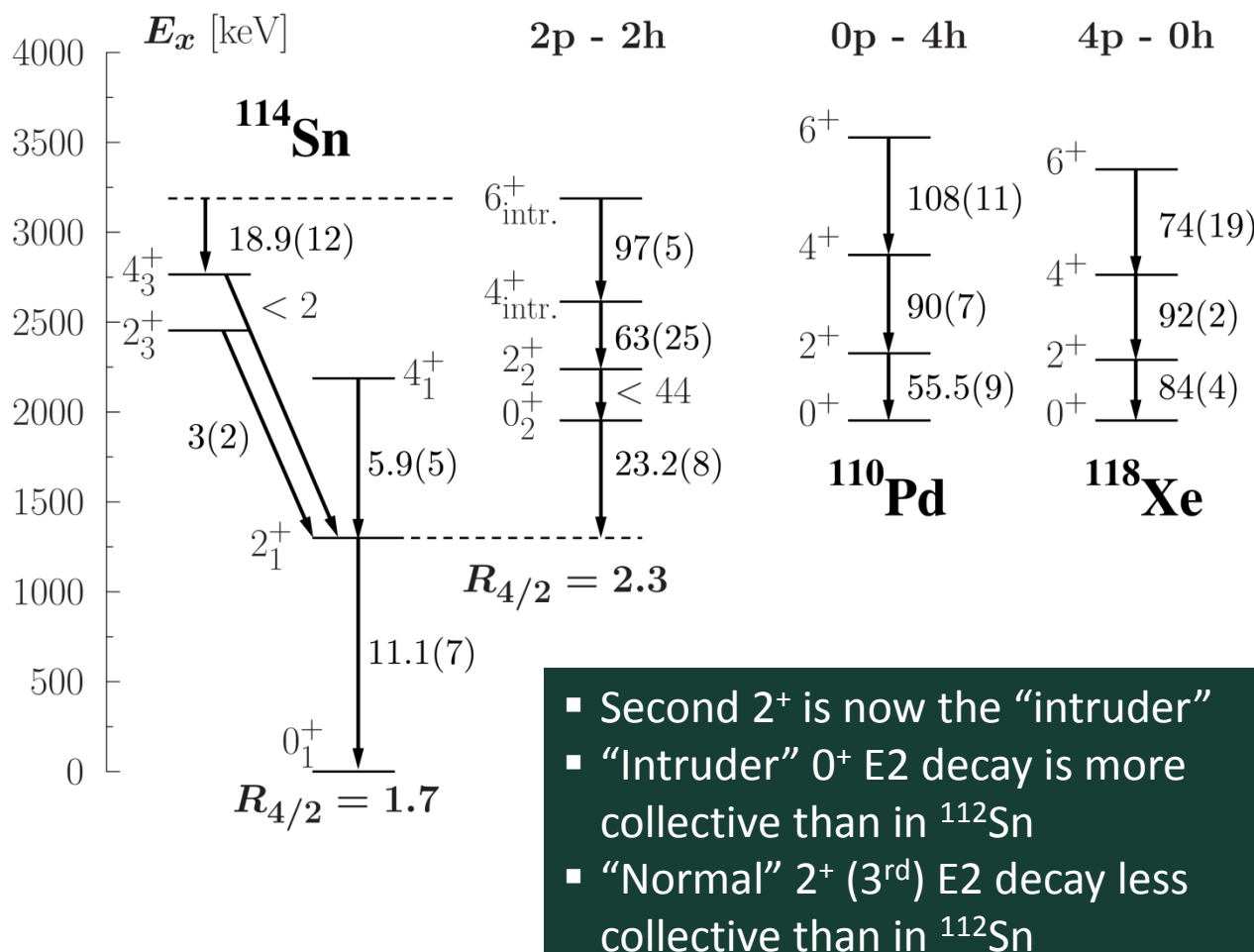
P.E. Garrett and J.L. Wood, J. Phys. G 37, 064028 (2010)



**Influence of underlying single-particle structure or overall structure change?**

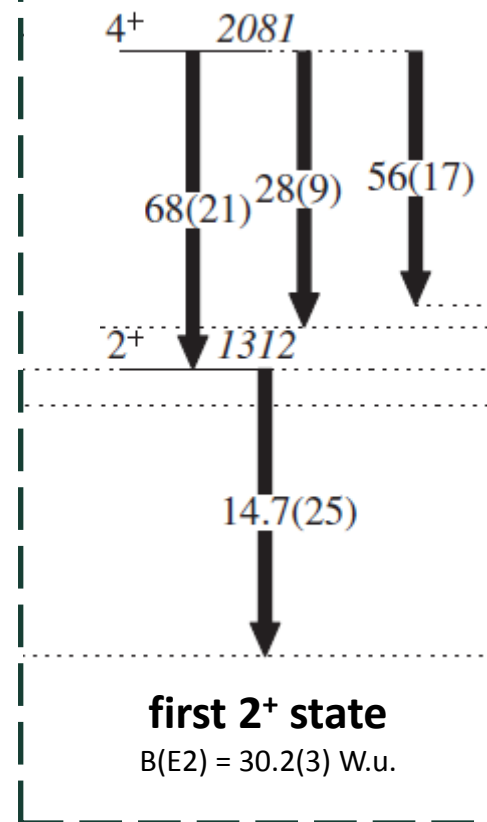
**Different influence of neutron single-particle states?**

# Shape coexistence in $^{114}\text{Sn}$



**$^{112}\text{Cd}$**

P.E. Garrett and J.L. Wood,  
J. Phys. G 37, 064028 (2010)



**Influence of underlying single-particle structure or overall structure change?**

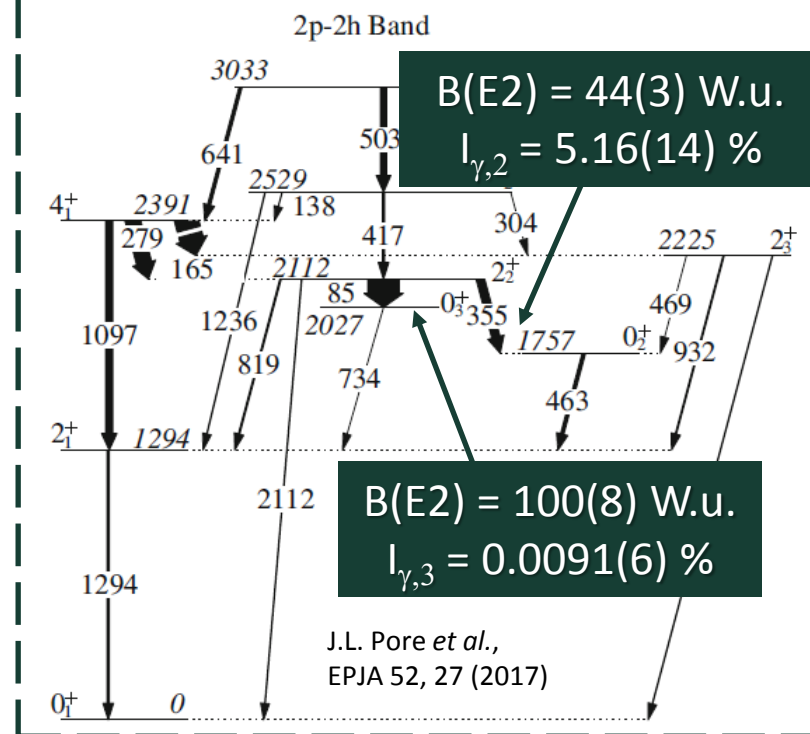
**Different influence of neutron single-particle states?**

# Shape coexistence in $^{114}\text{Sn}$

Comparison to IBM-2 mixing calculations  
(assuming  $^{110}\text{Pd}$  to cause intruder structure)

$J_i^\pi$	$E_x$ [MeV]	$E_{x,\text{IBM}}$ [MeV]	$J_f^\pi$	$B(E2)_{\text{exp.}} \downarrow$ [W.u.]	$B(E2)_{\text{IBM}} \downarrow$ [W.u.]
normal configuration					
$2_1^+$	1.30	1.30	$0_1^+$	11.1(7)	11
$4_1^+$	2.19	2.28	$2_1^+$	5.9(5)	19
$0_2^+$	1.95	1.99	$2_1^+$	23.2(8)	21
$2_3^+$	2.45	2.54	$0_1^+$	0.023(9)	0.004
			$2_1^+$	3(2)	17
			$2_2^+$	-	8
intruder configuration					
$0_3^+$	2.16	2.15	$2_1^+$	$\leq 5$	2
$2_2^+$	2.24	2.46	$0_1^+$	$\leq 0.12$	0.04
			$2_1^+$	$\leq 8$	2
			$0_2^+$	$\leq 44$	31
			$0_3^+$	-	27
$4_2^+$	2.61	3.00	$2_1^+$	6.6(10)	0.2
			$4_1^+$	1.6(10)	0.06
			$2_2^+$	62(25)	85
$6^+$	3.19	3.63	$4_1^+$	1.68(9)	1.5
			$4_2^+$	97(5)	93
			$4_3^+$	18.9(12)	0.7

## $^{116}\text{Sn}$ – Is 3<sup>rd</sup> 0<sup>+</sup> bandhead?



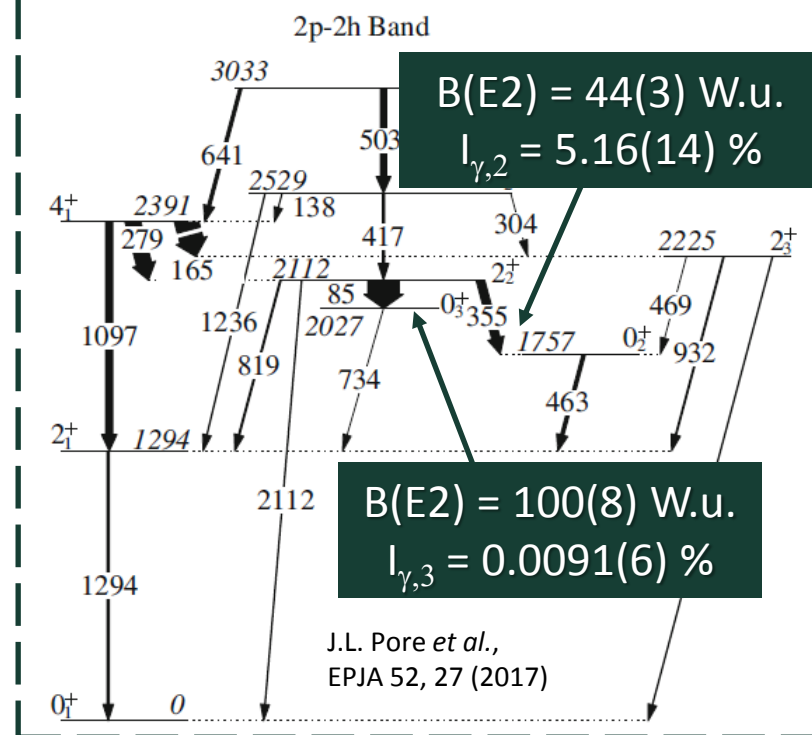


# Shape coexistence in $^{114}\text{Sn}$

Comparison to IBM-2 mixing calculations  
(assuming  $^{110}\text{Pd}$  to cause intruder structure)

$J_i^\pi$	$E_x$ [MeV]	$E_{x,\text{IBM}}$ [MeV]	$J_f^\pi$	$B(E2)_{\text{exp.}} \downarrow$ [W.u.]	$B(E2)_{\text{IBM}} \downarrow$ [W.u.]
normal configuration					
$2_1^+$	1.30	1.30	$0_1^+$	11.1(7)	11
$4_1^+$	2.19	2.28	$2_1^+$	5.9(5)	19
$0_2^+$	1.95	1.99	$2_1^+$	23.2(8)	21
$2_3^+$	2.45	2.54	$0_1^+$	0.023(9)	0.004
			$2_1^+$	3(2)	17
			$2_2^+$	-	8
intruder configuration					
$0_3^+$	2.16	2.15	$I_{\gamma,2} = 0.9(3) \% \text{ (Exp.)}$ $I_{\gamma,3} \approx 0.002 \% \text{ (IBM)}$		
$2_2^+$	2.24	2.46			
			$0_2^+$	$\leq 44$	31
			$0_3^+$	-	27
$4_2^+$	2.61	3.03	$B(E2) = 55.5(9) \text{ W.u. in } ^{110}\text{Pd}$		
			$2_1^+$	62(25)	85
$6^+$	3.19	3.63	$4_1^+$	1.68(9)	1.5
			$4_2^+$	97(5)	93
			$4_3^+$	18.9(12)	0.7

## $^{116}\text{Sn}$ – Is 3<sup>rd</sup> 0<sup>+</sup> bandhead?

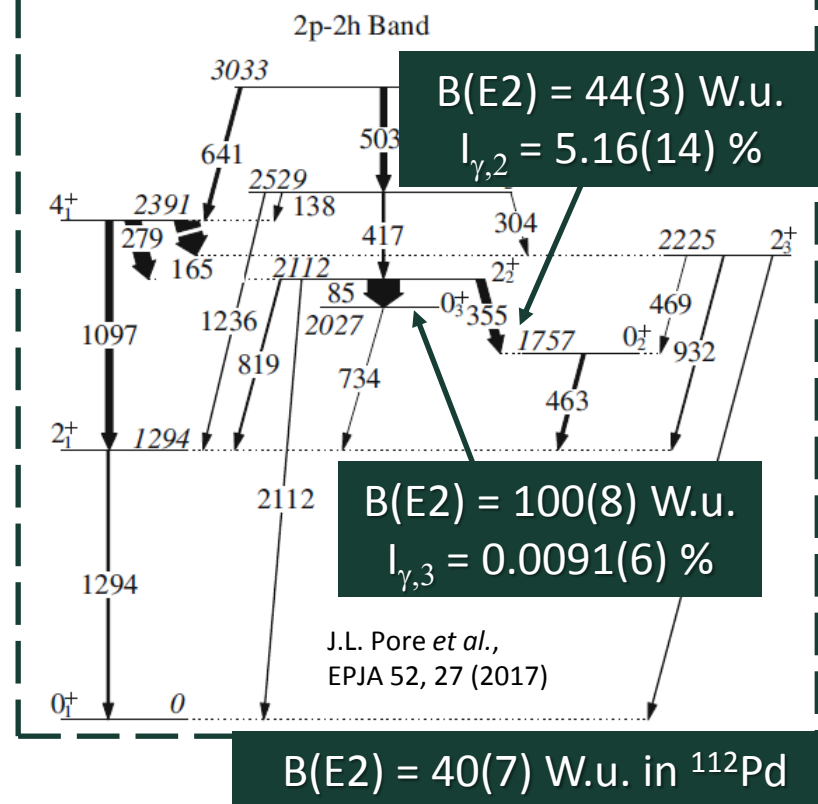


# Shape coexistence in $^{114}\text{Sn}$

Comparison to IBM-2 mixing calculations  
(assuming  $^{110}\text{Pd}$  to cause intruder structure)

$J_i^\pi$	$E_x$ [MeV]	$E_{x,\text{IBM}}$ [MeV]	$J_f^\pi$	$B(E2)_{\text{exp.}} \downarrow$ [W.u.]	$B(E2)_{\text{IBM}} \downarrow$ [W.u.]
normal configuration					
$2_1^+$	1.30	1.30	$0_1^+$	11.1(7)	11
$4_1^+$	2.19	2.28	$2_1^+$	5.9(5)	19
$0_2^+$	1.95	1.99	$2_1^+$	23.2(8)	21
$2_3^+$	2.45	2.54	$0_1^+$	0.023(9)	0.004
			$2_1^+$	3(2)	17
			$2_2^+$	-	8
intruder configuration					
$0_3^+$	2.16	2.15	$I_{\gamma,2} = 0.9(3) \% \text{ (Exp.)}$ $I_{\gamma,3} \approx 0.002 \% \text{ (IBM)}$		
$2_2^+$	2.24	2.46			
			$0_2^+$	$\leq 44$	31
			$0_3^+$	-	27
$4_2^+$	2.61	3.03	$B(E2) = 55.5(9) \text{ W.u. in } ^{110}\text{Pd}$		
			$2_2^+$	62(25)	85
$6^+$	3.19	3.63	$4_1^+$	1.68(9)	
			$4_2^+$	97(5)	
			$4_3^+$	18.9(12)	0.7

## $^{116}\text{Sn}$ – Is 3<sup>rd</sup> 0<sup>+</sup> bandhead?



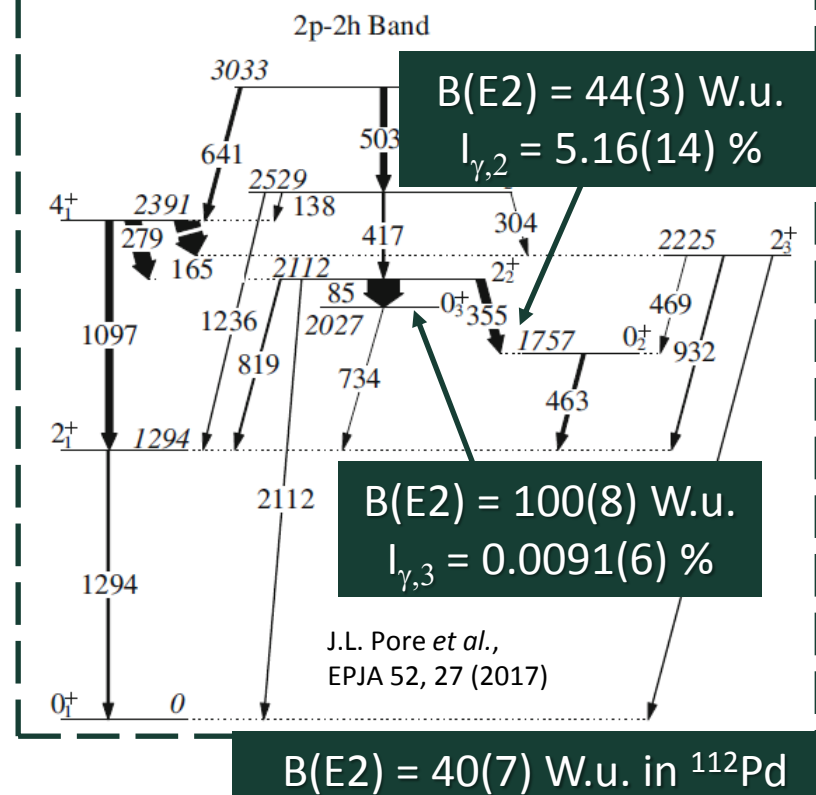
How could this large  $B(E2)$  in  $^{116}\text{Sn}$  be explained?

# Shape coexistence in $^{114}\text{Sn}$

Comparison to IBM-2 mixing calculations  
(assuming  $^{110}\text{Pd}$  to cause intruder structure)

$J_i^\pi$	$E_x$ [MeV]	$E_{x,\text{IBM}}$ [MeV]	$J_f^\pi$	$B(E2)_{\text{exp.}} \downarrow$ [W.u.]	$B(E2)_{\text{IBM}} \downarrow$ [W.u.]
normal configuration					
$2_1^+$	1.30	1.30	$0_1^+$	11.1(7)	11
$4_1^+$	2.19	2.28	$2_1^+$	5.9(5)	19
$0_2^+$	1.95	1.99	$2_1^+$	23.2(8)	21
$2_3^+$	2.45	2.54	$0_1^+$	0.023(9)	0.004
			$2_1^+$	3(2)	17
			$2_2^+$	-	8
intruder configuration					
$0_3^+$	2.16	2.15	$I_{\gamma,2} = 0.9(3) \% \text{ (Exp.)}$ $I_{\gamma,3} \approx 0.002 \% \text{ (IBM)}$		
$2_2^+$	2.24	2.46			
			$0_2^+$	$\leq 44$	31
			$0_3^+$	-	27
$4_2^+$	2.61	3.03	$B(E2) = 55.5(9) \text{ W.u. in } ^{110}\text{Pd}$		
			$2_2^+$	62(25)	85
$6^+$	3.19	3.63	$4_1^+$	1.68(9)	
			$4_2^+$	97(5)	
			$4_3^+$	18.9(12)	0.7

## $^{116}\text{Sn}$ – Is 3<sup>rd</sup> 0<sup>+</sup> bandhead?



How could this large  $B(E2)$  in  $^{116}\text{Sn}$  be explained?

$B(E2) = 101(5) \text{ W.u. in } ^{120}\text{Xe}$

# Summary

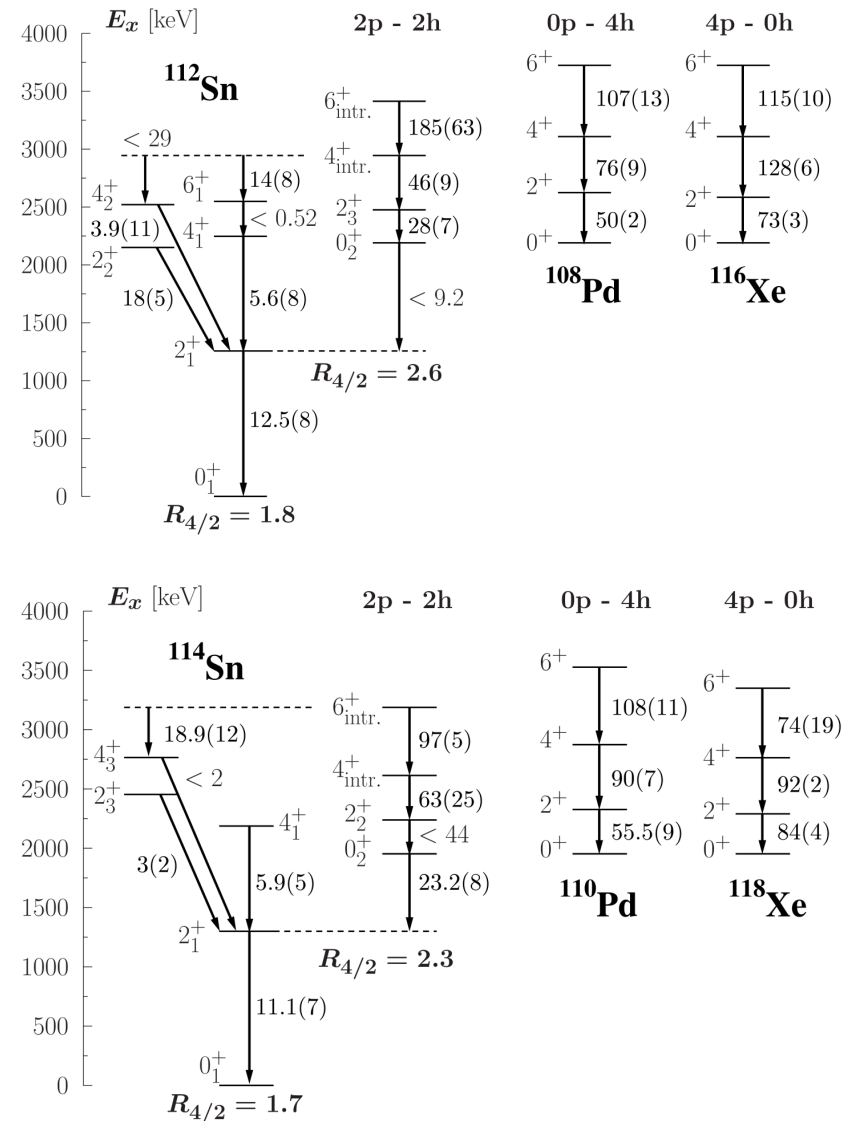
- **SONIC@HORUS** to determine lifetimes and  $\gamma$ -decay behavior of low-spin states via (p,p' $\gamma$ ) DSA coincidence technique

[A. Hennig *et al.*, NIM **794**, 171 (2015) ]

[S.G. Pickstone *et al.*, NIM **875**, 104 (2017)]

- **Collectivity of low-spin “intruder” states studied in  $^{112,114}\text{Sn}$**
- **Mixing hypothesis between normal and intruder configuration tested via schematic IBM-2 mixing calculations**
- **No clear hints at quadrupole multiphonon structures in  $^{112,114}\text{Sn}$**

[M. Spieker *et al.*, PRC **97**, 054319 (2018)]



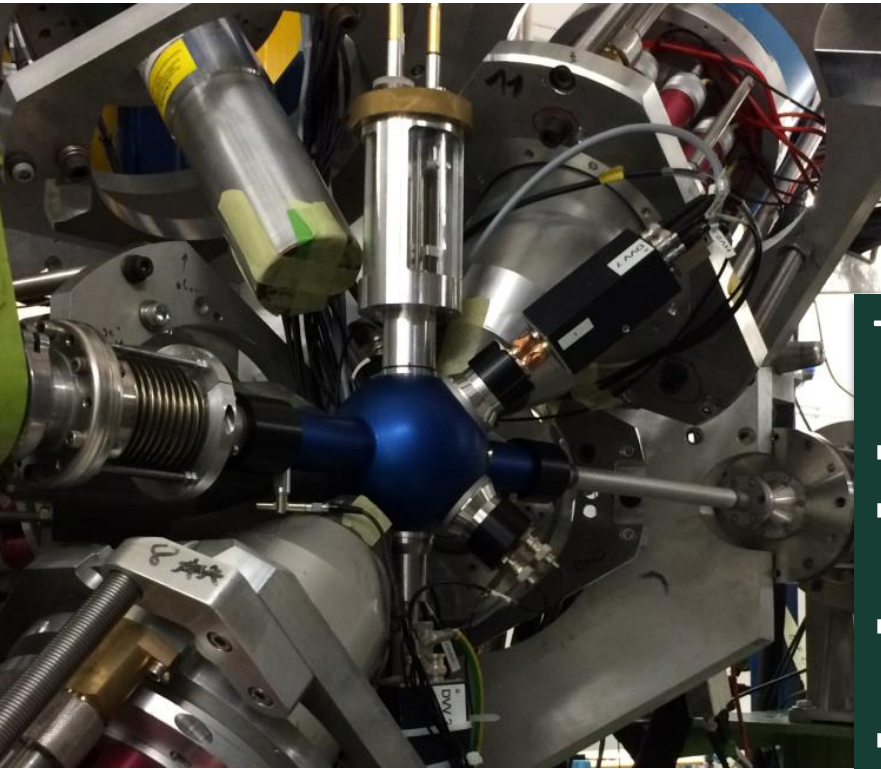


**back-up**



# (p,p'γ) DSA coincidence technique

Determination of γ-energy centroid shifts due to Doppler effect  
with SONIC@HORUS at UoC (Cologne, Germany)



$$E_{\gamma}(\Theta, t) = E_{\gamma}^0 \left( 1 + F(\tau) \frac{v_0}{c} \cos \Theta \right)$$

## The (p,p'γ) DSA coincidence technique

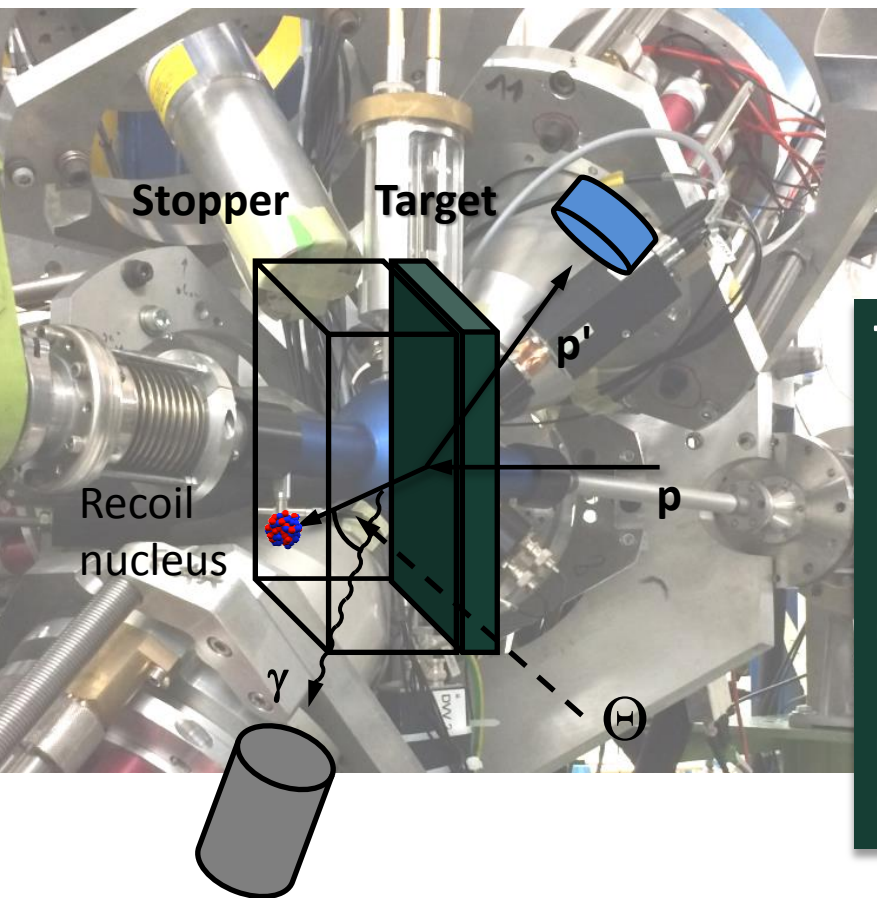
- Lifetimes from 10 fs to 1 ps can be measured
- Feeding from higher-lying states excluded due to pγ coincidences (excitation gate)
- γ-decay branching can be measured  
→ Partial decay widths accessible
- Dozens of lifetimes in one experiment!
- J = 0 – 6 are excited with (p,p') at E<sub>p</sub> = 8 MeV

(p,p'γ) DSA coincidence technique: A. Hennig *et al.*, NIM **794**, 171 (2015)

SONIC@HORUS (UoC, Germany): S.G. Pickstone *et al.*, NIM **875**, 104 (2017)

# (p,p'γ) DSA coincidence technique

Determination of γ-energy centroid shifts due to Doppler effect  
with SONIC@HORUS at UoC (Cologne, Germany)



$$E_{\gamma}(\Theta, t) = E_{\gamma}^0 \left( 1 + F(\tau) \frac{v_0}{c} \cos \Theta \right)$$

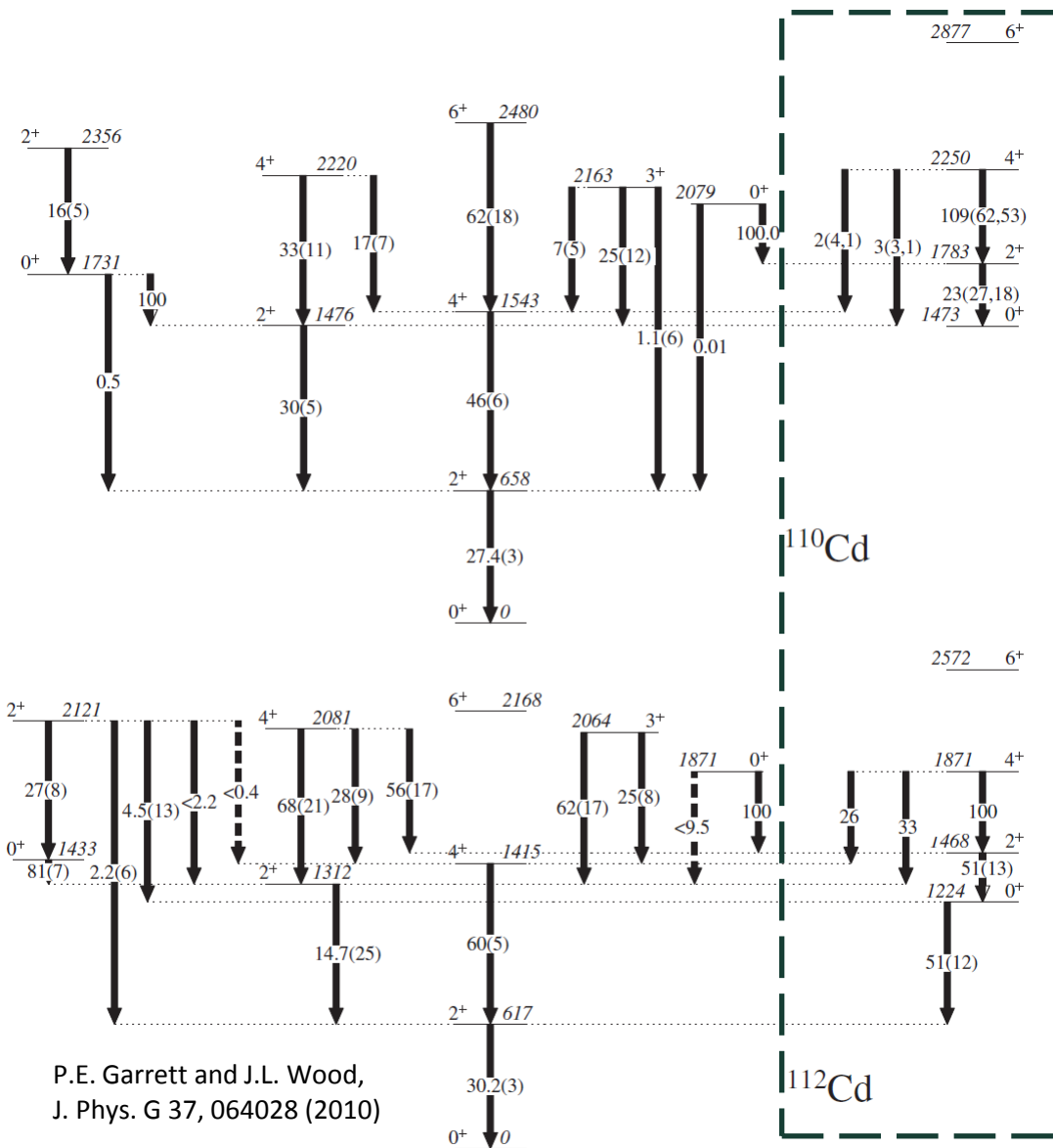
## The (p,p'γ) DSA coincidence technique

- Lifetimes from 10 fs to 1 ps can be measured
- Feeding from higher-lying states excluded due to pγ coincidences (excitation gate)
- γ-decay branching can be measured  
→ Partial decay widths accessible
- Dozens of lifetimes in one experiment!
- J = 0 – 6 are excited with (p,p') at E<sub>p</sub> = 8 MeV

(p,p'γ) DSA coincidence technique: A. Hennig *et al.*, NIM **794**, 171 (2015)

SONIC@HORUS (UoC, Germany): S.G. Pickstone *et al.*, NIM **875**, 104 (2017)

# Shape coexistence in Cd isotopes



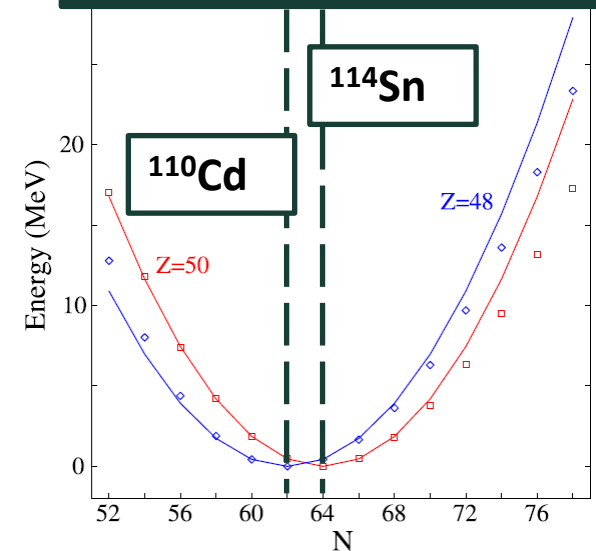
P.E. Garrett and J.L. Wood,  
J. Phys. G 37, 064028 (2010)

Shape coexistence in  $^{110,112}\text{Cd}$  ( $Z = 48$ ,  $N = 62, 64$ )

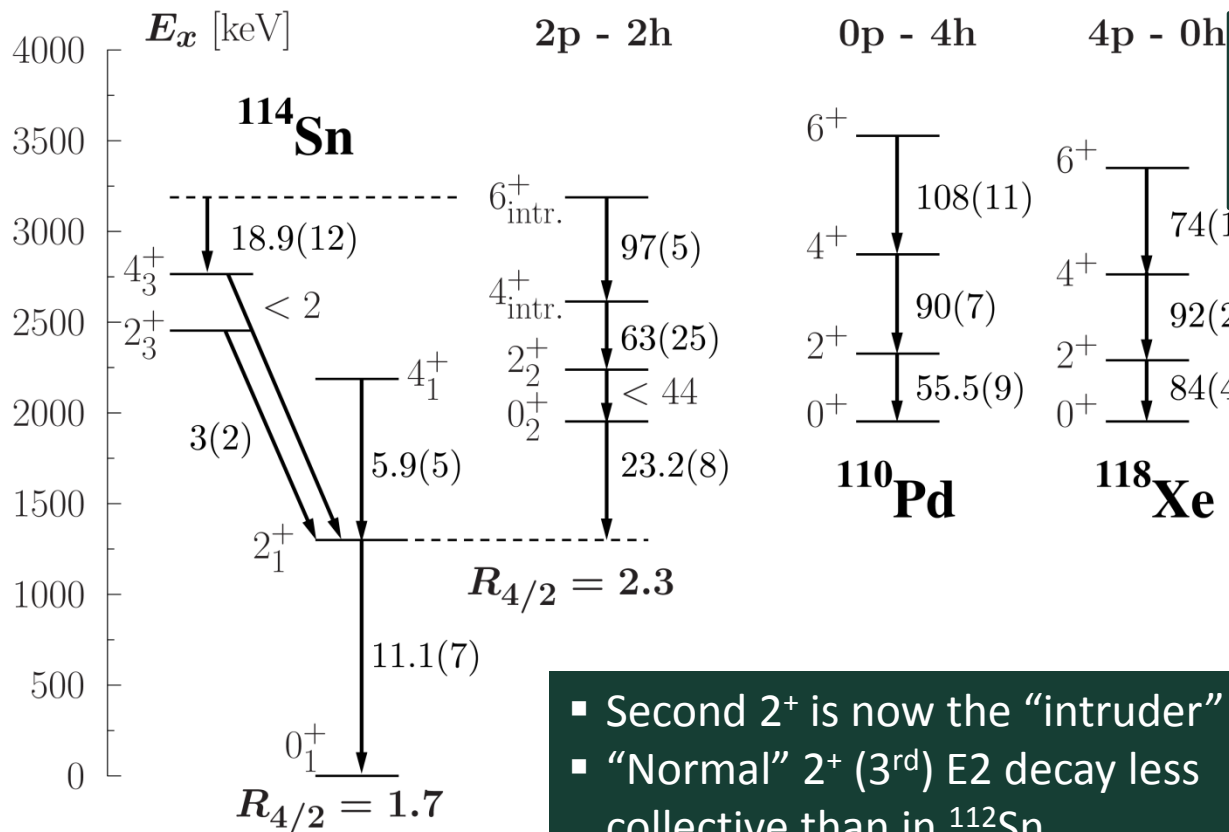
- “additional” states observed  
→ attributed to 2p-4h excitations across the  $Z = 50$  shell closure, i.e. Pd isotopes as “inert core”

P.E. Garrett, J. Phys. G 43, 084002 (2016)

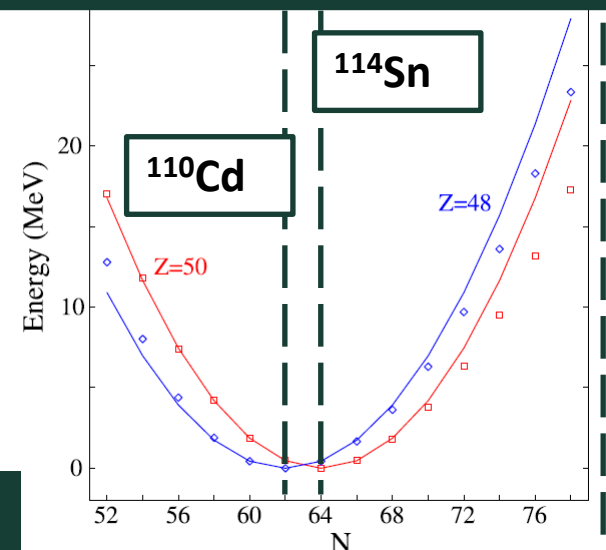
Ground-state energies  
compared to  
Pairing rotor model



# Shape coexistence in $^{114}\text{Sn}$



## Ground-state energies compared to Pairing rotor model



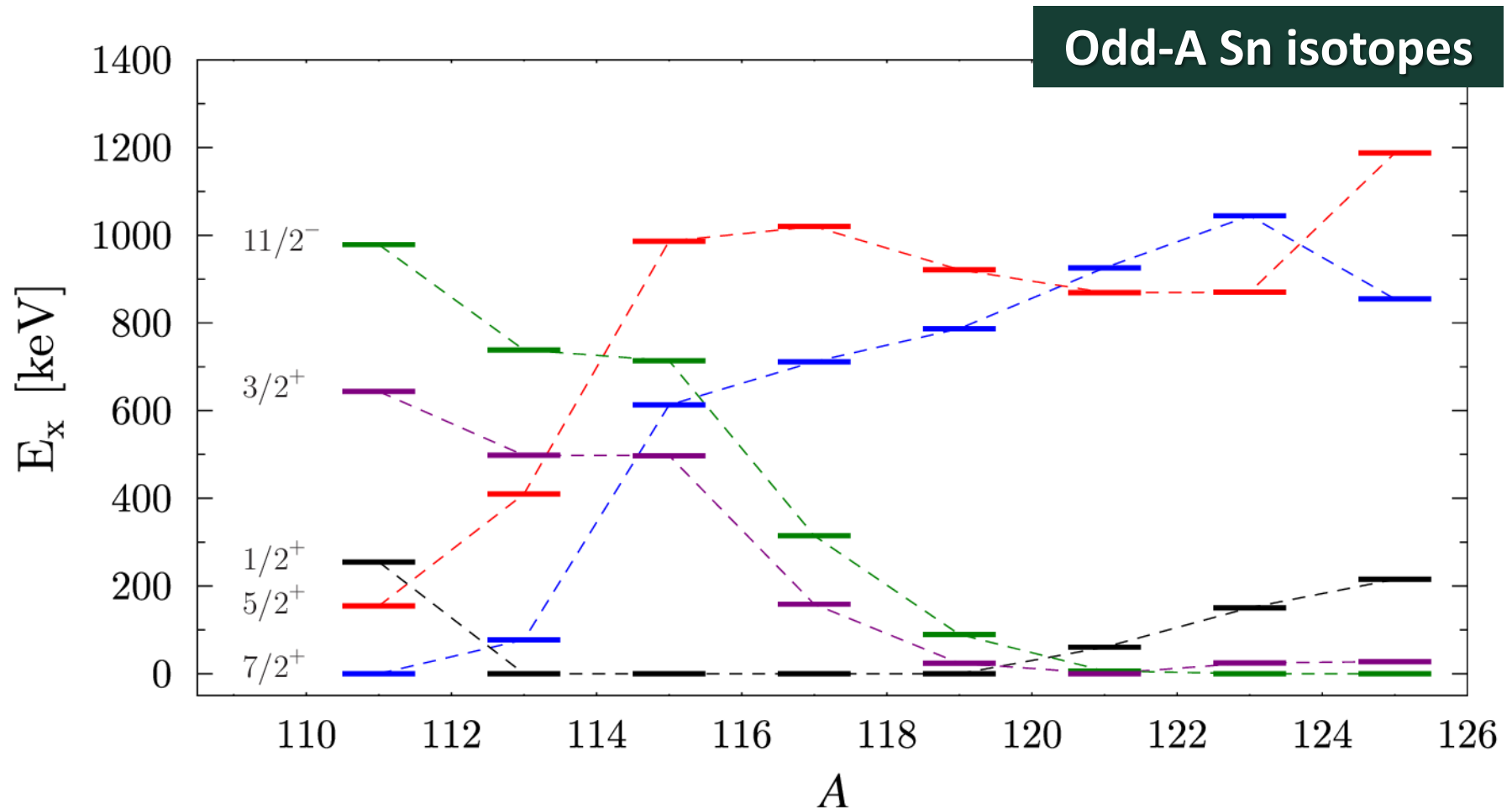
P.E. Garrett, J. Phys. G 43, 084002 (2016)

- Second  $2^+$  is now the “intruder”
- “Normal”  $2^+$  ( $3^{\text{rd}}$ ) E2 decay less collective than in  $^{112}\text{Sn}$
- “Intruder”  $0^+$  E2 decay is more collective than in  $^{112}\text{Sn}$

**Influence of underlying single-particle structure or overall structure change?**

**Different influence of neutron single-particle states?**

# Neutron single-particle structure



# Are there quadrupole multiphonon states?

$J_i^\pi$	$E_x$ [keV]	$J_f^\pi$	$B(E2)_{\text{exp.}}$ [W.u.]
$^{112}\text{Sn}$			
$0^+$	2617.4(3)	$2_1^+$	$\leq 2$
		$2_2^+$	$\leq 7$
$2^+$	2720.6(2)	$0_1^+$	$\leq 0.02$
		$2_1^+$	$0.06^{+0.08}_{-0.01}$
		$2_2^+$	$\leq 4.3$
		$0_2^+$	$3.3(12)$
$3^+$	2755.2(3)	$2_1^+$	$\leq 0.004$
		$2_2^+$	$\leq 12$
		$4_1^+$	$\leq 45$
		$4_2^+$	$\leq 0.2$
$4^+$	2783.5(2)	$2_1^+$	$5.1(6)$
		$4_1^+$	$\leq 35$
$^{114}\text{Sn}$			
$4^+$	2859.2(5)	$2_1^+$	$2.8(4)$
		$4_1^+$	$\leq 10$
		$2_2^+$	$< 5$
		$2_3^+$	$< 46$
$2^+$	2943.4(2)	$0_1^+$	$< 0.001$
		$2_1^+$	$\leq 0.3$
		$0_2^+$	$\leq 0.4$
		$2_2^+$	$\leq 0.9$
		$0_4^+$	$\leq 1.6$
		$2_3^+$	$\leq 5.2$
$0^+$	3028.0(2)	$2_1^+$	$1.7(7)$
		$2_2^+$	$1.4(10)$
		$2_3^+$	$16(8)$

## $^{124}\text{Sn}$

D. Bandyopadhyay *et al.*, NPA **747**, 206 (2005)

$J_i^\pi$ [ $\hbar$ ]	$J_f^\pi$ [ $\hbar$ ]	Exp [W.u.]
$2_1^+$	$0_1^+$	$9.0^a$
$4_1^+$	$2_1^+$	$4.8^a$
$2_2^+$	$2_1^+$	$< 9.3$
$2_2^+$	$0_1^+$	$< 0.004$
$0_2^+$	$2_1^+$	$< 8.3$
$0_3^+$	$2_2^+$	$< 78$
$0_3^+$	$2_1^+$	$< 1.6$
$2_3^+$	$2_2^+$	$4.4^{+0.2}_{-4.4}$
$2_3^+$	$2_1^+$	$0.12^{+0.13}_{-0.07}$
$2_3^+$	$0_1^+$	$0.028^{+0.008}_{-0.007}$
$6_1^+$	$4_1^+$	$< 90$
$3_1^+$	$4_2^+$	$< 46^b$
$3_1^+$	$4_1^+$	$< 5$
$3_1^+$	$2_2^+$	$< 67^b$
$3_1^+$	$2_1^+$	$< 0.3$
$4_3^+$	$4_2^+$	$3.1^{+14}_{-3.1}$
$4_3^+$	$4_1^+$	$4.2^{+0.2}_{-0.2}$
$4_3^+$	$2_1^+$	$0.27^{+0.21}_{-0.19}$

<sup>a</sup> Calculated using the halflives from Ref. [14].

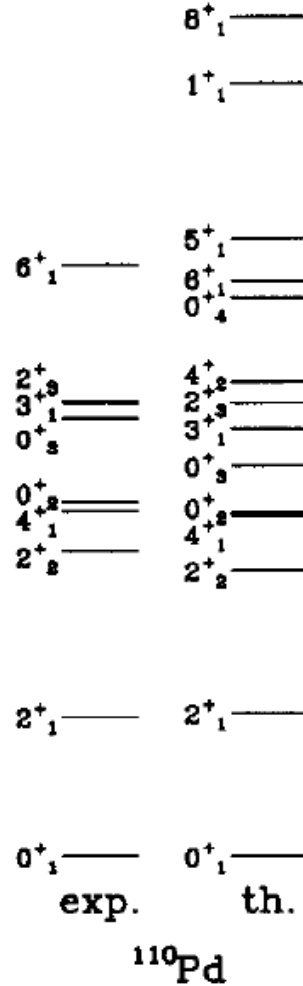
<sup>b</sup> Calculated using mixing ratios from the present work and from Ref. [20].



# IBM-2 calculations

Table IV. Comparison of the normal and intruder configurations identified experimentally and the predictions of the *sd* IBM-2 with mixing in  $^{114}\text{Sn}$ . The parameters for the intruder configuration were adopted from Ref. [53], i.e.  $^{110}\text{Pd}$ . The parameters for the normal configuration in  $^{114}\text{Sn}$  were adopted from Ref. [54] but slightly changed, i.e.  $C_{0\nu} = -0.55$ ,  $C_{2\nu} = 0$ , and  $C_{4\nu} = -0.31$ . The mixing parameters  $\alpha$  and  $\beta$  were kept at 0.2 and 0, respectively.  $\Delta$ , i.e. the relative energy shift between the normal and intruder configurations was set to 2.78 MeV. The parameters of the *E2* operator were also slightly changed to  $e_\nu = 0.07\text{eb}^2$ ,  $e_\pi = 0.105\text{eb}^2$  and  $e_2/e_0 = 1.43$ . The experimental  $B(E2; 2_1^+ \rightarrow 0_1^+)$  value is taken from Ref. [35]. For a description of the Hamiltonian, the *E2* operator and their parameters see, *e.g.*, Refs. [53, 55].

$J_i^\pi$	$E_x$ [MeV]	$E_{x,\text{IBM}}$ [MeV]	$J_f^\pi$	$B(E2)_{\text{exp.}} \downarrow$ [W.u.]	$B(E2)_{\text{IBM}} \downarrow$ [W.u.]
normal configuration					
$2_1^+$	1.30	1.30	$0_1^+$	11.1(7)	11
$4_1^+$	2.19	2.28	$2_1^+$	5.9(5)	19
$0_2^+$	1.95	1.99	$2_1^+$	23.2(8)	21
$2_3^+$	2.45	2.54	$0_1^+$	0.023(9)	0.004
			$2_1^+$	3(2)	17
			$2_2^+$	-	8
intruder configuration					
$0_3^+$	2.16	2.15	$2_1^+$	$\leq 5$	2
$2_2^+$	2.24	2.46	$0_1^+$	$\leq 0.12$	0.04
			$2_1^+$	$\leq 8$	2
			$0_2^+$	$\leq 44$	31
			$0_3^+$	-	27
$4_2^+$	2.61	3.00	$2_1^+$	6.6(10)	0.2
			$4_1^+$	1.6(10)	0.06
			$2_2^+$	62(25)	85
$6^+$	3.19	3.63	$4_1^+$	1.68(9)	1.5
			$4_2^+$	97(5)	93
			$4_3^+$	18.9(12)	0.7



## Hamiltonian:

$$H = \epsilon_\pi n_{d_\pi} + \epsilon_\nu n_{d_\nu} + \kappa Q_\pi \cdot Q_\nu + M_{\pi\nu} + V_{\pi\pi} + V_{\nu\nu}$$

## Parts of Hamiltonian:

$$Q_\rho = (d^\dagger \times s + s^\dagger \times \tilde{d})_\rho^{(2)} + \chi_\rho (d^\dagger \times \tilde{d})_\rho^{(2)}, \quad \rho = \pi, \nu,$$

$$M_{\pi\nu} = \frac{1}{2} \xi_2 (s_\nu^\dagger \times d_\pi^\dagger - d_\nu^\dagger \times s_\pi^\dagger)^{(2)} \cdot (s_\nu \times \tilde{d}_\pi - \tilde{d}_\nu \times s_\pi)^{(2)} \\ + \sum_{k=1,3} \xi_k (d_\nu^\dagger \times d_\pi^\dagger)^{(k)} \cdot (\tilde{d}_\pi \times \tilde{d}_\nu)^{(k)}$$

( $\kappa$  and  $\xi$ s are 0 for  $^{114}\text{Sn}$ )

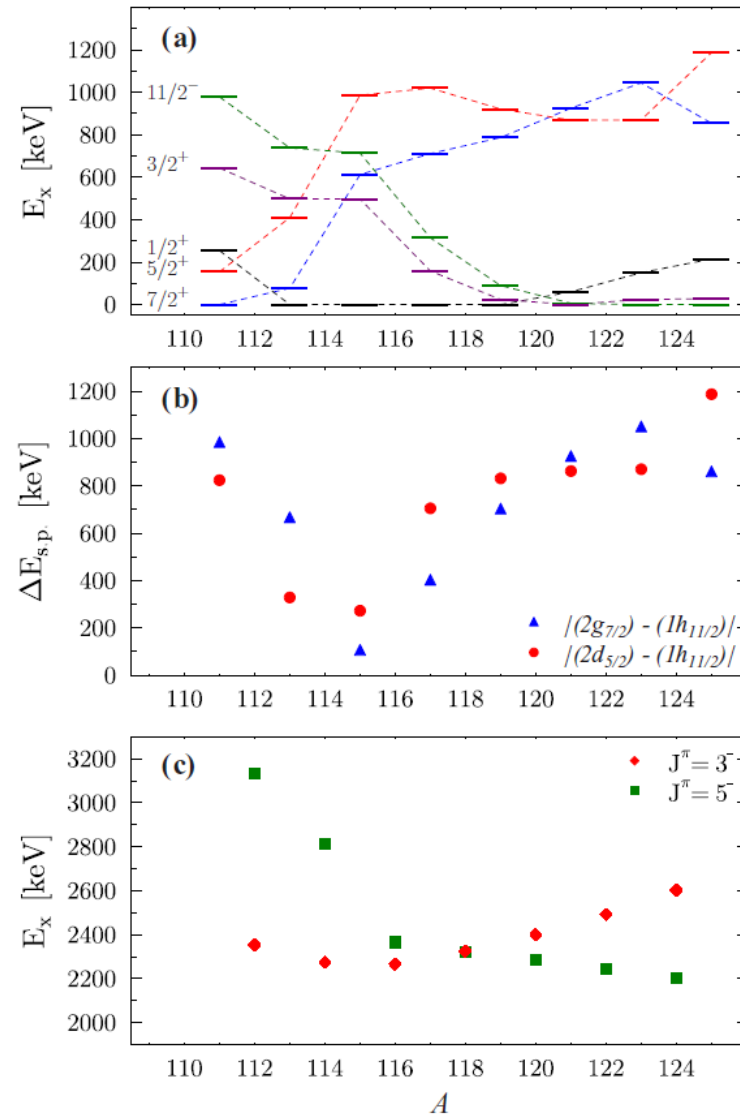
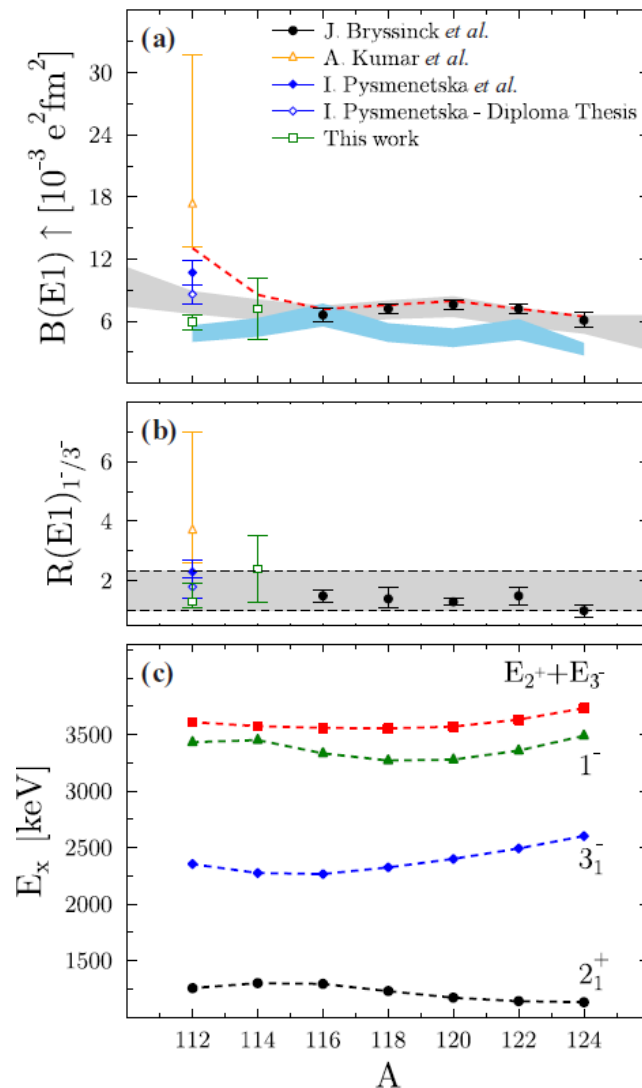
$$V_{\rho\rho} = \sum_{L=0,2,4} \frac{1}{2} c_L^\rho (d_\rho^\dagger \times d_\rho^\dagger)^{(L)} \cdot (\tilde{d}_\rho \times \tilde{d}_\rho)^{(L)}, \quad \rho = \pi, \nu$$

## Mixing part:

$$H_{\text{mix}} = \alpha (s_\pi^\dagger s_\pi^\dagger + s_\pi s_\pi)^{(0)} + \beta (d_\pi^\dagger d_\pi^\dagger + \tilde{d}_\pi \tilde{d}_\pi)^{(0)}$$

$^{110}\text{Pd}$ : K.H. Kim *et al.*, NPA **604**, 163 (1996)

# Quadrupole-octupole coupled states



# $^{112}\text{Sn}$ : Quadrupole-octupole coupled states

$E_x$ [keV]	$J^\pi$	$J_f^\pi$	$E_f$ [keV]	$E_\gamma$ [keV]	$I_\gamma$	$B(E1) \downarrow$ [mW.u.]	$B(E2) \downarrow$ [W.u.]
1256.5(2)	$2_1^+$	$0_1^+$	0	1256.5(2)	1		$12.5(7)^a$
2353.7(2)	$3_1^-$	$2_1^+$	1256.5(2)	1097.2(2)	1	1.13(8)	
3383.3(2)	$3^-$	$2_1^+$	1256.5(2)	2126.8(2)	0.85(2)	0.120(9)	
		$2_2^+$	2150.5(3)	1232.9(2)	0.041(9)	0.030(7)	
		$(2^+, 3, 4^+)$	2917.0(2)	466.5(2)	0.11(2)	1.5(2)	
3396.6(2)	$2^{(-)}$	$2_1^+$	1256.5(2)	2139.9(2)	0.057(13)	0.005(2)	
		$2_2^+$	2150.5(2)	1246.1(2)	0.64(3)	0.30(9)	
		$3_1^-$	2353.7(2)	1042.4(2)	0.27(5)		$9_{-7}^{+3}$
		$2_4^+$	2720.6(2)	675.8(2)	0.039(9)	0.11(5)	
3433.4(2)	$1^{(-)}$	$0_1^+$	0	3433.4(2)	1	1.31(15)	
3497.9(2)	$5^-$	$3_1^-$	2353.7(2)	1144.2(2)	0.70(4)		29(13)
		$4_2^+$	2520.5(2)	977.1(2)	0.27(6)	0.39(18)	
		$4^+$	2783.5(2)	714.7(3)	$\leq 0.03$	$\leq 0.19$	
3553.2(2)	$(3)^-$	$2_1^+$	1256.5(2)	2296.8(2)	0.83(3)	0.06(2)	
		$3_1^+$	2755.2(3)	797.7(3)	0.17(3)	0.30(10)	
3827.1(3)	$(1^-, 2^+)$	$0_1^+$	0	3827.1(2)	0.58(3)	0.040(5)	
		$2_1^+$	1256.5(2)	2570.8(2)	0.29(5)	0.066(11)	
		$3_1^-$	2353.7(2)	1473.0(7)	0.13(3)		4.5(11)
3984.7(3)	$(1^-, 2^+)$	$0_1^+$	0	3984.7(3)	0.79(2)	0.08(2)	
		$3_1^-$	2353.7(2)	1630.0(3)	0.14(2)		5(2)
		$2_3^+$	2475.5(2)	1507.8(4)	0.07(2)	0.137(95)	

# $^{114}\text{Sn}$ : Quadrupole-octupole coupled states

$E_x$ [keV]	$J^\pi$	$J_f^\pi$	$E_f$ [keV]	$E_\gamma$ [keV]	$I_\gamma$	$B(E1) \downarrow$ [mW.u.]	$B(E2) \downarrow$ [W.u.]
1299.7(2)	$2_1^+$	$0_1^+$	0	1299.7(2)	1		$11.1(7)^a$
2274.5(2)	$3_1^-$	$2_1^+$	1299.7(2)	974.8(2)	1	0.65(8)	
2814.6(2)	$5_1^-$	$4_1^+$	2187.3(3)	627.4(2)	0.88(2)	$\leq 0.77$	
		$3_1^-$	2274.5(2)	539.9(2)	0.12(3)		$\leq 38$
2904.9(3)	$3^-$	$2_1^+$	1299.7(2)	1605.1(4)	0.026(5)	0.0030(14)	
		$4_1^+$	2187.3(3)	717.3(2)	0.77(2)	0.7(3)	
		$3_1^+$	2514.4(2)	390.2(2)	0.20(3)	1.6(7)	
		$4_2^+$	2613.7(4)	290.3(4)	0.011(4)	0.21(12)	
3225.1(2)	$3^-$	$2_1^+$	1299.7(2)	1925.4(2)	0.920(14)	0.11(2)	
		$2_3^+$	2453.8(2)	771.4(4)	0.019(7)	0.04(2)	
		$3^-$	2904.9(3)	319.9(4)	0.061(13)		
3397.3(2)	$3^-$	$2_1^+$	1299.7(2)	2097.6(2)	0.31(5)	0.06(2)	
		$2_2^+$	2238.6(2)	1158.3(2)	0.13(2)	0.14(6)	
		$3_1^-$	2274.5(2)	1122.0(4)	0.44(2)		$3_{-3}^{+11}$
		$2_3^+$	2453.8(2)	943.2(2)	0.12(2)	0.24(10)	
3452.1(2)	$(1^-)$	$0_1^+$	0	3452.1(2)	1	1.6(7)	
3483.9(4)	$(1^-, 2^+)$	$2_1^+$	1299.7(2)	2184.1(2)	0.671(13)	0.06(2)	
		$0_3^+$	2155.9(2)	1327.7(3) <sup>b</sup>	0.094(14)	0.037(11)	
		$3_1^-$	2274.5(2)	1209.0(2)	0.235(14)		5.2(13)
3514.1(3)	$3^-$	$2_1^+$	1299.7(2)	2214.4(2)	0.76(3)	0.14(6)	
		$4_1^+$	2187.4(3)	1327.0(4) <sup>c</sup>	0.07(2)	0.06(3)	
		$2_2^+$	2238.6(2)	1275.0(3)	0.17(3)	0.17(8)	
3524.4(2)	$3^-$	$2_1^+$	1299.7(2)	2224.5(3)	0.55(3)	0.023(17)	
		$4_1^+$	2187.3(3)	1158.3(2)	0.15(3)	0.028(22)	
		$3_1^-$	2274.5(2)	1122.0(4)	0.13(2)		1.2(10)
		$2_3^+$	2453.8(2)	943.2(2)	0.17(3)	0.08(6)	
3610.2(4)	$5^{(-)}$	$4_1^+$	2187.3(3)	1422.9(3)	1	1.0(3)	
3650.3(3)	$(1^-, 2^+)$	$0_1^+$	0	3650.1(3)	0.44(3)	0.012(4)	
		$2_1^+$	1299.7(2)	2350.3(3)	0.11(2)	0.011(5)	
		$0_3^+$	2155.9(2)	1493.7(3)	0.09(2)	0.04(2)	
		$3_1^-$	2274.5(2)	1374.6(2)	0.36(6)		6(2)